

## ABSTRACT

Title of Document: THE CARIBBEAN LOW-LEVEL JET:  
ITS STRUCTURE AND INTERANNUAL  
VARIABILITY

Ernesto Muñoz, Doctor of Philosophy, 2007

Directed By: Professor Antonio J. Busalacchi,  
Earth System Science Interdisciplinary Center

The Caribbean region shows maxima in easterly winds greater than 12 m/s at 925 hPa in July and February referred herein as the summer and winter Caribbean low-level jet (CBNLLJ), respectively. The purpose of this study is to identify the mechanisms of the CBNLLJ formation and variability and their association to the regional hydroclimate. To study the climatological aspects of the CBNLLJ, climatological fields are calculated from 1979 to 2001. It is observed that the low-level (925-hPa) zonal wind over the Caribbean basin has a semi-annual cycle. The semi-annual cycle has peaks in February and July that are regional amplifications of the large-scale circulation by means of a meridional pressure gradient. High mountains to the south of the Caribbean Sea influence the air temperature meridional gradient providing a baroclinic structure that favors a stronger easterly wind. The boreal summer strengthening of the CBNLLJ is associated with subsidence over the subtropical North Atlantic from the May-to-July evolution of the Central American

monsoon. Additionally, the mid-summer minimum of Caribbean precipitation is related to the Caribbean LLJ through greater moisture flux divergence.

The CBNLLJ has interannual variability with greater standard deviation during boreal summer. The summer interannual variability of the CBNLLJ is due to variability of the meridional pressure gradient across the Caribbean basin influenced by sea surface temperature (SST) gradients between the tropical Pacific and the tropical Atlantic. To determine the inter-decadal changes statistical diagnostics of summer CBNLLJ anomalies are analyzed for different periods, in particular 1958-1978 and 1979-2001. Also analyzed were inter-basin SLP and SST gradient indices. The CBNLLJ showed more intense events and greater persistence during 1979-2001 than during 1958-1978 as a result of more extreme SLP and SST inter-basin gradients during the more recent decades. These are due to changes in the relation between the Pacific and the Atlantic after the late 1970's. The results of the present study are important in the context of understanding an intrinsic component of the Caribbean climate, i.e., the Caribbean low-level jet.

THE CARIBBEAN LOW-LEVEL JET:  
ITS STRUCTURE AND INTERANNUAL VARIABILITY

By

Ernesto Muñoz

Dissertation submitted to the Faculty of the Graduate School of the  
University of Maryland, College Park, in partial fulfillment  
of the requirements for the degree of  
Doctor of Philosophy  
2007

Advisory Committee:  
Professor Antonio J. Busalacchi, Chair  
Professor Sumant Nigam  
Professor James Carton  
Professor Hugo Berbery  
Dr. Alfredo Ruiz-Barradas  
Professor Ruth DeFries, Dean's Representative

© Copyright by  
Ernesto Muñoz  
2007

## Foreword

In this Ph.D. thesis by Ernesto Muñoz the annual and interannual variability of the Caribbean Low-Level Jet (CBNLLJ) is analyzed. Over the past forty years an extensive literature has developed for the meridionally-oriented and land-based Great Plains Low-Level Jet and South American Low-Level Jet that serve as moisture corridors from low latitudes into central North and South America, respectively. In contrast, relatively little is known about what controls the variability of the zonally-oriented low-level jet over the Caribbean Sea and its role in the regional hydroclimate. In this thesis and subsequent journal articles the seasonal variability of the CBNLLJ is shown to be influenced by changes to the Bermuda High to the north and the orography of South America on its southern flank. Seasonal fluctuations of the CBNLLJ control the downstream bifurcation of moisture transport into either Central America or the Gulf of Mexico. On interannual time scales, zonal pressure gradients and related sea surface temperature anomalies between the tropical Pacific and tropical Atlantic exert strong control on CBNLLJ fluctuations. Since the late 1970's the influence of the tropical Pacific has increased to the extent that there have been more extreme and longer lasting CBNLLJ events in late summer. The results of this work have important implications for understanding the mechanisms that govern precipitation variability in the region, moisture transport to remote regions, and ultimately the predictability of both.

*Antonio J. Busalacchi*

Antonio J. Busalacchi  
Professor and Director  
Earth System Science Interdisciplinary Center

## Acknowledgements

I thank Prof. Antonio J. Busalacchi for his role as advisor and for all his support during my Ph.D. track.

I thank the ESSIC personnel: Eric Hackert, Mark Baith and James Beauchamp for facilitating the computing aspect of my job, and Linda Carter and Karen MacKey for facilitating the administrative aspect of my years in ESSIC.

I thank the dissertation committee for their time and helpful discussions.

Thanks to Prof. Nigam and Dr. Ruiz-Barradas for their facilitation of the data from NARR and ERA-40.

Also, thanks to the professors with whom I took classes for sharing with me their knowledge.

I thank the UCAR Significant Opportunities in Atmospheric Research and Science (SOARS) Program for their support during my first year of graduate school.

I thank my wife for her unconditional support throughout graduate school.

## Table of Contents

Foreword.....	ii
Acknowledgements .....	iii
Table of Contents .....	iv
List of Tables.....	v
List of Figures .....	vi
Chapter 1 : Introduction and Objectives .....	1
1.1 Motivation .....	1
1.2 Objectives and outline of this study.....	4
Chapter 2 : Background .....	6
2.1 Caribbean annual climate and the Caribbean low-level jet.....	6
2.2 Other American low-level jets.....	12
2.3 Remote influences on the tropical North Atlantic and Caribbean regions.....	14
2.4 Tropical and North Atlantic relation to Caribbean precipitation.....	20
Chapter 3 : Methodology .....	25
3.1 The Data .....	25
3.2 Hypotheses and Approach.....	28
3.2.1 Seasonal Variability .....	28
3.2.2 Interannual Variability .....	31
Chapter 4 : Climatology.....	34
4.1 Introduction .....	34
4.2 The Caribbean low-level jet .....	36
4.2.1 Seasonal and diurnal variability.....	36
4.2.2 Horizontal and vertical structure.....	39
4.2.3 Caribbean moisture flux structure and seasonal cycle .....	44
4.3 Summer climate and the Caribbean LLJ.....	48
4.3.1 Onsets of the Caribbean LLJ .....	48
4.3.2 Summer Caribbean minimum of precipitation .....	51
Chapter 5 : Interannual Variability and Changes .....	58
5.1 Summer interannual variability .....	58
5.2 Changes in the Caribbean LLJ strength and persistence.....	68
5.3 Changes in the remote forcing of the Caribbean LLJ .....	73
Chapter 6 : Conclusions .....	82
6.1 Climatological features .....	82
6.2 Interannual variability and changes .....	84
6.3 Future work .....	86
Bibliography.....	88

## List of Tables

Table 5.1. Sea level pressure anomaly (SLPA) indices .....	73
Table 5.2. Sea surface temperature anomaly (SSTA) indices.....	73



## List of Figures

Figure 2.1. Annual mean of the 925-hPa wind from ERA-40. The reference arrow is 10 m/s.....	7
Figure 4.1. February (left) and July (right) climatology of 925-hPa winds from the NARR (top) and the ERA-40 (bottom). The base period is from 1979 to 2001. The reference arrow is 10 m/s. The shadings correspond to the magnitude of the vectors in m/s. Vectors with speed less than 3 m/s are not shown. The limits of the NARR domain are observed in the bottom left and bottom right corners of its plots. The rectangle delineates the area of the maximum wind speed from 12°N to 16°N and from 71°W to 76°W. ....	37
Figure 4.2. Vertical profile of the zonal wind (m/s) averaged for the column 71°W-76°W and 12°N-16°N from the NARR (top) and the ERA-40 (bottom) for the calendar months. Negative indicates easterly.....	38
Figure 4.3. Pressure-time plot of the February (a) and July (b) diurnal cycle of the zonal wind (m/s) at 13°N and 74°W from the NARR. ....	39
Figure 4.4. February (a) and July (b) climatology of sea level pressure (hPa) from the ERA-40. ....	40
Figure 4.5. Pressure-latitude cross-section of February (left) and July (right) zonal total wind, temperature and thermal wind averaged from 71°W to 76°W from NARR. Top panels: Zonal component of the wind (m/s). Negative indicates easterly. Middle panels: Temperature (K, dark contours) and the departure from the meridional (11°N-to-19°N) mean of temperature (K, shadings). Bottom panels: Zonal thermal wind (m/s). Thermal wind values greater than 0.25 (solid contours) are shaded in dark gray while values less than -0.25 (dashed contours) are shaded in light gray. The mountains of South America are observed at 11°N while the mountains of the Greater Antilles are observed at 19°N. ....	41
Figure 4.6. Pressure-latitude cross-sections and seasonal cycle of moisture flux from NARR. Top panels: Zonal moisture flux (m/s·g/kg) averaged from 71°W to 76°W for (a) February and (b) July. The mountains of northern South America and the Greater Antilles are shaded. Middle panels: Magnitude of the moisture flux vector (m/s·g/kg) averaged from 80°W to the eastern side of the mountains of Central America or to 93°W for (c) February and (d) July. The dashed line indicates where the meridional moisture flux is zero. The mountains of Central America are shaded in the background. Mountains shaded lighter are to the west of 88°W. Bottom panel: Annual cycle of the moisture flux (m/s·g/kg) averaged from 80°W to the eastern side of the mountains of Central America or to 93°W and vertically integrated from 700 hPa to 1000 hPa. The moisture flux vector is represented by arrows and the magnitude is shaded. The dashed line is the zero-meridional moisture flux. ....	45
Figure 4.7. Annual cycle of the 71°-76°W zonal average of (a) sea level pressure (hPa, contour interval of 2 hPa) and (b) 925-hPa zonal wind (m/s, contour interval of 1.5 m/s) from NARR. The Greater Antilles are at about 19°N and South America at 11°N. ....	48

Figure 4.8. June-May difference of the irrotational wind and its divergence (left panels) and of the rotational wind and its vorticity (right panels) at 250 hPa (upper panels) and 925 hPa (lower panels) from the NCEP/NCAR Reanalysis. Reference arrow in m/s. Negative values are shaded. A reference line has been drawn from 20°N, 70°W to 30°N, 50°W. Contour interval for the difference in divergence is  $2 \text{ s}^{-1} \times 10^{-6}$ , for the difference in vorticity at 250 hPa is  $4 \text{ s}^{-1} \times 10^{-6}$  and at 925 hPa is  $3 \text{ s}^{-1} \times 10^{-6}$ .....51

Figure 4.9. (a) July precipitation (mm/day), (b) vertical pressure velocity at 850 hPa ( $\text{Pa/s} \times 100$ ) and (c) sea surface temperature ( $^{\circ}\text{C}$ ). The rectangle delineates the area from 12°N to 16°N and from 71°W to 76°W. ....53

Figure 4.10. (a) July-May difference of precipitation (mm/day) from GPCP. Contour interval is 1 mm/day. (b) Pressure-longitude cross-section of the July-May difference of diabatic heating ( $\text{K/s} \times 10^5$ , shades) and the zonal and vertical wind (streamlines) averaged from 12°N to 16°N from ERA-40. In (b) the mountains of Central America are in white between 85°W and 90°W. ....55

Figure 4.11. Correlation between the 12-month seasonal cycle of precipitation and the 12-month seasonal cycle of Caribbean 925-hPa zonal wind index. The precipitation is from GPCP. The Caribbean 925-hPa zonal wind index (multiplied by -1) is the area-average between 12°N and 16°N and between 71°W and 76°W from NARR. Correlation coefficients significant at the 95% level are shown. ....57

Figure 5.1. June-to-September average standard deviation of the 925-hPa zonal wind anomalies (m/s) from NARR (shades) and ERA-40 (contours).....58

Figure 5.2. Time series (bars) of Caribbean LLJ anomalies (m/s) for June, July and August from ERA-40.....59

Figure 5.3. July 925-hPa wind anomaly vector (m/s, top) and SLPA (hPa, bottom) regressed onto the Caribbean LLJ July anomaly index (i.e., 925-hPa zonal wind anomalies averaged over 12-17°N and 70-80°W). Contour interval of SLPA is 0.2 hPa. Negative SLPA are dashed contours and positive SLPA are solid contours. Values statistically significant at the 95% level are shaded. The regions in the equatorial Pacific, Caribbean and equatorial Atlantic indicated by a rectangle in the bottom figure were used for area-averages of SLPA. ....60

Figure 5.4. May (top), July (middle) and September (bottom) SSTA ( $^{\circ}\text{C}$ ) regressed onto July CBNLLJ anomaly index. Contour interval is  $0.1^{\circ}\text{C}$ ..... 62

Figure 5.5. July (left) rotational and (right) irrotational component of the wind (m/s) and (left) streamfunction ( $1/\text{s}$ ) and (right) velocity potential ( $1/\text{s}$ ) anomalies regressed onto July Caribbean LLJ anomaly index. Top panels are for 250-hPa level and bottom panels are for 925-hPa level. A reference arrow is displayed at the top of each panel. Negative anomalies are dashed contours and positive anomalies are solid contours. Contour interval of 250-hPa streamfunction is  $1\text{e}+6$ ; of 925-hPa streamfunction is  $4\text{e}+5$ ; of 250-hPa velocity potential is  $2\text{e}+5$ ; of 925-hPa velocity potential is  $2\text{e}+5$ . ....64

Figure 5.6. July precipitation anomaly (mm) regressed onto the CBNLLJ July anomaly index. Contours are -0.3, -0.1, 0.1 and 0.3. Positive (negative) precipitation anomalies are solid (dashed) contours. Values statistically significant at the 95% level are shaded. Precipitation data is from ERA-40. ....65

Figure 5.7. Correlation between July CBNLLJ anomalies and the North Atlantic Oscillation index (NAO; violet bars) or the Niño3.4 index (blue bars) during previous, concurrent and posterior months. ....	66
Figure 5.8. Autocorrelation of July Caribbean LLJ anomalies with summer months for two different periods: 1958-1978, 1981-2001. A line showing the 99% significance level is shown. ....	69
Figure 5.9. Twenty-one-year running standard deviation (m/s) of CBNLLJ anomalies for June, July, August and September. ....	70
Figure 5.10. Histograms of June-July (top) and August-September (bottom) CBNLLJ anomalies between the periods 1958-1978 (left) and 1979-2001 (right). The x-axis indicates the value of the center of the bin (e.g., 0 for the bin from -0.5 to 0.5). The y-axis indicates the percentage of events for each bin. ....	71
Figure 5.11. Twenty-one-year correlation between SLP standardized anomalies of the equatorial Pacific and the Caribbean for (top) June, July; and (middle) August, September. (bottom) Twenty-one-year correlation between SST standardized anomalies of the equatorial Pacific and the tropical North Atlantic for June, July, August and September. Solid lines are concurrent correlations. Dashed lines are correlations with the Pacific index leading the Atlantic index. ....	75
Figure 5.12. SLPA (hPa) regressed to CBNLLJ anomaly index for (top) June, (middle) July and (bottom) August for the periods (left) 1958-1978 and (right) 1979-2001. Negative anomalies are dashed contours and positive anomalies are solid contours. Contour interval is 3 hPa for June, 0.2 hPa for July and 2 hPa for August. Shaded areas indicate values significant at the 95% level. ....	77
Figure 5.13. Same as previous figure but for SSTA (°C). Contour interval is 1°C for June, 0.1°C for July and 1°C for August. ....	79
Figure 5.14. Regions of 80% significant difference (shaded) between the correlations for the periods 1958-1978 and 1979-2001 for SLPAs and CBNLLJ (left) and SSTAs and CBNLLJ (right). ....	80
Figure 5.15. June, June-July and June-August 21-year running standard deviation of Tahiti station SLPAs. The square on each line indicates the value for the 21-year period centered on 1978. ....	81

## Chapter 1 : Introduction and Objectives

### 1.1 Motivation

Low-level jets (LLJs) are regional maxima in winds in the lower troposphere (Paegle, 1998). The LLJs play an important role in the exchange of atmospheric water vapor from upwind to downwind regions (Nogues-Paegle and Paegle, 2000). Two examples of LLJs are the Great Plains LLJ (GPLLJ) and the South American LLJ (SALLJ). Many studies have documented the GPLLJ and the SALLJ having formulated a few hypotheses for their existence. These low-level jets are important for their potential to transport moisture from remote upwind regions, for their relation to nighttime convection, and for their potential to alter the convergent and divergent circulations on interannual timescales.

Stensrud (1996) indicated the western Caribbean Sea as an area where a low-level atmospheric jet is suspected to exist. The date of that publication indicates that until recently the existence of an atmospheric low-level jet in the Caribbean still required proof or proper documentation. In fact, it was not until 2007 that a few studies were published that explicitly document the atmospheric jet in the Caribbean and some aspects of its annual and interannual variability. Recently, Muñoz et al. (2007) analyzed the climatological features of the Caribbean Low-Level Jet (CBNLLJ) in July and February. Muñoz et al. (2007) also presented evidence that supports the remote forcing of the CBNLLJ inter-annual variability by the Atlantic and Pacific basins. Wang (2007) presented the interannual correlation between the CBNLLJ and SLP, SST and precipitation in August-September and January-February (from the

early 1950s to the early 2000s). Wang (2007) also presents the correlation of climate variables with the Great Plains LLJ. Additionally, Whyte et al. (2007) analyzed the CBNLLJ by a combined EOF analysis of Caribbean zonal wind and tropical SSTs (from the early 1950s to the late 1990s). Whyte et al (2007) also present the correlation of the CBNLLJ with precipitation, but they limit their discussion to mentioning the regions with highest correlation.

There are still unknowns about the regional influences of the LLJ in the Caribbean and its forcing, either local or remote. This study focuses on the annual and interannual variability of the LLJ over the Caribbean Sea and its relation to the regional and larger-scale climate.

The Caribbean region shows a maximum in zonal wind in boreal summer at 925 hPa. This maximum has been associated with a low-level atmospheric jet and named CBNLLJ. In addition to the summer maximum in July there is a secondary maximum in February and a minimum in October. Mo et al (2005) identified a summer maximum of surface zonal winds over the region (12-14°N, 70-80°W) and associated it to the CBNLLJ. However, even though there is a region of strong winds at the surface, the atmospheric column over the Caribbean Sea has maximum zonal winds at about 925 hPa. Also, the diurnal cycle of the CBNLLJ has not been documented even though it may be related to convection variability throughout the day.

Given its strong winds and its flow over the Intra-Americas Sea (IAS), i.e. the Caribbean Sea and the Gulf of Mexico, the CBNLLJ may enhance evaporation and increase the moisture content of the air transported away from the region. The CBNLLJ has a central branch heading to Central America and a northern branch that

shifts northward flowing over the Yucatan Peninsula and the Yucatan Channel leading to the Gulf of Mexico. Previous studies found the Gulf of Mexico to be a moisture source for the continental United States (Helfand and Schubert, 1995; Bosilovich and Schubert, 2002) while about 50% of the total water vapor imported into Gulf of Mexico comes from the Caribbean Sea region (Hastenrath, 1966; Rasmusson, 1967). Mestas-Nuñez et al (2005) confirmed that the IAS is a moisture source exporting mainly to the west and to the north. Hence, quantifying the moisture transport of the CBNLLJ is pivotal in understanding the moisture sources of Central America and to the west, and the Gulf of Mexico, among other regions.

In fact, the CBNLLJ seems to play a significant role in the hydroclimate of the Caribbean and Central America. The precipitation annual cycle in the Caribbean and Central American region has a rainy season in boreal summer (Giannini et al, 2000). Taylor et al (2002) observed that for years when the precipitation in the late rainy season (August-October) is higher than average, the CBNLLJ is weaker over Central America. However, the mechanisms by which the CBNLLJ affects the regional precipitation are still unclear. Through modulation of moisture flux convergence and vertical wind shear, the CBNLLJ may be a key atmospheric modulator of precipitation and convection anomalies in the Intra-Americas Sea (IAS) region (i.e., the Caribbean Sea and the Gulf of Mexico regions). Nonetheless, the potential mechanisms by which the CBNLLJ influences the regional hydroclimate have not been addressed.

The peak of the CBNLLJ and its variability coincide with the period when the regional precipitation is most pronounced and when the Caribbean Sea and the Gulf

of Mexico are in their warm pool phase. Several studies have focused on the variability of the Intra-Americas Sea warm pool and its effect on convection, precipitation and hurricanes (Wang et al, 2001; 2006). Due to the easterly orientation of the CBNLLJ and its position to the north of South America, the CBNLLJ has the capacity to induce coastal upwelling throughout the southern boundary of the Caribbean Sea.

The CBNLLJ also seems to be subject to remote influences. Mora and Amador (2000) observed that for El Niño events the CBNLLJ intensifies while for La Nina events the CBNLLJ weakens. Magaña (2000) linked a stronger CBNLLJ during Pacific El Niño years to negative precipitation anomalies over Central America. These observations lead me to hypothesize that the CBNLLJ is one of the features by which teleconnections are exerting their influence on the precipitation of the Caribbean and Central America regions. However, how or what mechanisms control the response of the CBNLLJ to remote influences such as El Niño-Southern Oscillation is unknown. Other remote phenomena that may influence the variability of the CBNLLJ are the North Atlantic Oscillation and the variability of the tropical Atlantic.

### 1.2 Objectives and outline of this study

Several questions about the CBNLLJ and its climate interactions stand out. How is the CBNLLJ related to its regional climate during the annual cycle? What leads to the onset of the CBNLLJ? Does the CBNLLJ have a strong diurnal cycle? On seasonal timescales, is the CBNLLJ related to precipitation and to moisture fluxes over the Caribbean and Central American region? How do the CBNLLJ anomalies

relate to Intra-Americas Sea SSTAs and to non-regional (Pacific and Atlantic) SSTAs? Answering these questions would advance our knowledge of the CBNLLJ and the role of the CBNLLJ on the climate of the regions affected by it.

Based on the previous discussion the following objectives will be addressed by this study.

- Characterize the climatological structure of the Caribbean zonal winds and determine the factors that control it.
- Determine the mechanisms that regulate the interannual variability of the summer CBNLLJ.

Through achieving these objectives I intend to answer the questions stated above. The next chapters of the dissertation will address the following. Chapter 2 will examine the historical background of the Caribbean climate and its low-level jet. The basic Caribbean climate will be described with particular focus on the summer conditions. Aside from the discussion of the Caribbean Low-Level Jet, other low-level jets will be discussed as background. Then, the influences of the remote ENSO phenomenon on the Caribbean climate will be described, followed by a discussion of climate interactions in the vicinity of the Caribbean region. Chapter 3 will present the data sets and the approach used to study the Caribbean Low-Level Jet. The results will be separated into two chapters: one dedicated to the analyses of the climatology (Chapter 4) and another one (Chapter 5) dedicated to the analyses of the interannual variability of the CBNLLJ. Chapter 6 is dedicated to state the conclusions of the study. Additionally, future research will be discussed.



## Chapter 2 : Background

### 2.1 Caribbean annual climate and the Caribbean low-level jet

The Caribbean Sea is bounded to the south by South America, to the west by Central America, to the east by the Lesser Antilles and to the north by the Greater Antilles. The Gulf of Mexico is to the northwest of the Caribbean Sea connected by the Yucatan Channel. During summer, the Caribbean region is characterized by the presence of a warm pool with SSTs greater than 28.5°C, a rainy season from May to October, strong low-level easterly flow and hurricane activity.

As observed from the annual mean of low-level (925-hPa) winds (Fig. 2.1), the Caribbean Sea region has strong easterly winds throughout the lower troposphere that seem to be an extension of the northeasterly trades. This strong low-level flow with its core at about 925 hPa and its signal at the surface has been named the Caribbean Low-level Jet (CBNLLJ; Mo et al, 2005) and the Intra-Americas Low-level Jet (Amador and Mo, 2005). The flow has a central branch heading towards Central America and a northwestward branch heading towards the Gulf of Mexico. The central branch encounters the Central American cordillera and is blocked by the mountainous regions, but goes through the major gaps having as extensions the gap winds of Central America and their associated jets, in particular the Papagayo Jet through the Lake Nicaragua gap (Xie et al, 2005).

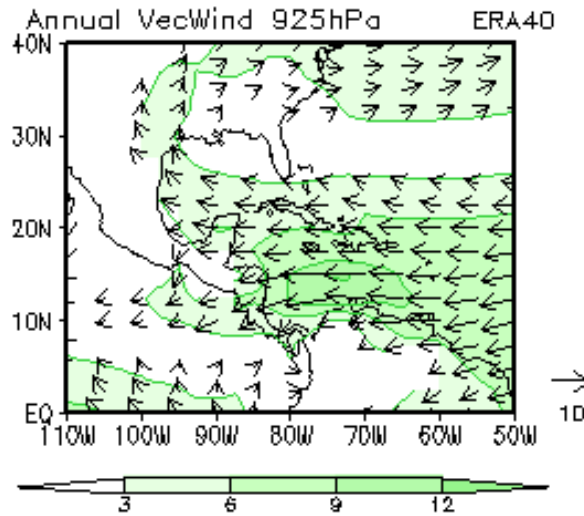


**Figure 2.1.** Annual mean of the 925-hPa wind from ERA-40. The reference arrow is 10 m/s.

These connections between the North Atlantic trade winds, the CBNLLJ and the extensions to the Gulf of Mexico and over Central America may vary together or with lags and leads from month to month or from year to year. These connections raise questions such as the following. Is the CBNLLJ related to the subtropical North Atlantic High? How does the northwestern branch of the CBNLLJ change when the central branch strengthens? To what extent are the gap winds over Central America associated to the CBNLLJ?

The strongest Caribbean winds of June and July flow over warm water of about 27°C. In the Gulf of Mexico SSTs are greater than 28.5°C during July and August. When the easterly winds over the Caribbean Sea weaken in August, the 28.5°C SST isotherm extends to include the Caribbean Sea. The area of the Caribbean Sea and the Gulf of Mexico (i.e., the Intra-Americas Sea) and the North Tropical Atlantic with SSTs greater than 28.5°C has been dubbed the Intra-Americas Sea (IAS) warm pool

or Atlantic warm pool (AWP; Wang et al, 2006) and peaks during September. Separated by Central America, the IAS warm pool has a counterpart in the northeastern tropical Pacific (NETP) which peaks earlier in the year during April-May (Wang and Enfield, 2001; 2003).

Albeit the presence of water warmer than 28.5°C over both the Eastern Pacific Warm Pool and the Intra-Americas Sea Warm Pool, the precipitation during the rainy season has distinctive patterns on either side of Central America. Over and to the west of Central America (over the eastern Pacific warm pool) convective activity is intense, constituting the Intertropical Convergence Zone; while at the same latitudes to the east of Central America (over the IAS warm pool) tropical convection is relatively weak. Overall, in the Caribbean and Central American region, the rainy season is in boreal summer and the dryer season in winter (Giannini et al, 2000). The rainy season has two maxima, one in June and another in September, divided by a relative minimum in July-August (Magaña et al, 1999; Giannini et al, 2000). This relative minimum during the middle of the summer has been named mid-summer drought (Magaña et al, 1999) and is referred to as the *canícula*.

Magaña et al. (1999) explained the *canícula* over Mexico and Central America as a result of the feedback between SST, convection, cloudiness, and the strength of the easterlies. After the initial increase of SST during early summer, convection is triggered and cloudiness increase, initiating the early rainy season. Later, the strengthening of the easterlies (at 925 hPa) during mid-summer induces convection over the eastern side of Central America and divergence and subsidence over the western side of Central America. The strengthening of the easterlies is concurrent

with a decrease in SST over the eastern Pacific warm pool region. These changes result in the *canícula* with a decrease of precipitation over the western side of Central America and clear skies. Magaña et al. (1999) speculated that an increase in shortwave radiation (due to clear skies coincidental with the *canícula*) increases SST which then leads to greater convection and the start of the late rainy season. This second maximum of precipitation is also due to a weakening of the 925-hPa easterlies according to Magaña et al. (1999). These interactions and the associated changes of the 925-hPa easterly winds point to the importance of the CBNLLJ in the modulation of the *canícula*, the precipitation over Central America and even the SSTs over the western side of Central America. As the CBNLLJ changes intensity from year to year, these interactions may vary and result in longer dry periods or the absence of the *canícula* in some summers.

Previous studies have analyzed the atmospheric moisture budget over the Gulf of Mexico and Caribbean Sea (Hastenrath, 1966; Rasmusson, 1967, 1968, 1971). In summary, Hastenrath (1966) and Rasmusson (1967, 1968, 1971) found that the Caribbean Sea local evaporation minus precipitation (E-P) accounts for about a fifth of the total water vapor source. Also, the total water vapor exported from the Caribbean Sea represents about half of the total water vapor imported to the Gulf of Mexico. They also found that summer (July-September) is when the meridional moisture flux from the IAS into the United States peaks. During the summer is when the CBNLLJ peaks and due to its potential influence on the moisture fluxes to the Gulf of Mexico it merits further study.

Mestas-Nuñez et al (2005), after averaging the moisture fluxes bounded by the Intra-Americas Sea (IAS, i.e., the Caribbean Sea and Gulf of Mexico), indicated that the IAS is a moisture sink (as it precipitates in the basin) from August through October with a minimum in September and a source from October through August with a maximum in February. Mestas-Nuñez et al (2005) also find that the Gulf of Mexico is a source year round with a minimum in September and maximum in November. The Caribbean region is a source from December through July with maximum in March, and a sink from August through November with a minimum in October (Mestas-Nuñez et al, 2005). Hence, during summer the IAS is a sink of atmospheric moisture, but the Caribbean changes its role from being a source in July to being a sink in August. Nonetheless, what is the role of the CBNLLJ in the moisture fluxes away from the Caribbean? Understanding the CBNLLJ and its moisture transport will help to understand a source of moisture for the Gulf of Mexico and the continental United States, and a source of moisture for Central America and to the west, among other regions.

The recent advent of a few studies on the CBNLLJ provides a basic description of the jet. Recently, in a study analyzing the reliability of the North American Regional Reanalysis (NARR) from the National Center for Environmental Prediction (NCEP), Mo et al (2005) presented boreal summer climatologies of the surface zonal winds of the Caribbean. Mo et al (2005) explained that the major branch of moisture transport to the United States is carried by the CBNLLJ from the tropical Atlantic to the Gulf of Mexico and then is transported by the Great Plains LLJ from the Gulf of Mexico to the central United States. Also using NARR data, Amador and Mo (2005) identify

the CBNLLJ and indicate that the CBNLLJ has two maxima throughout the year: one in July and another in February. Wang and Lee (2007) also identified the seasonal cycle of the CBNLLJ. Amador and Mo (2005) identify the jet maximum at 925 hPa near 12-17°N and 70-80°W.

Nonetheless, the controls on the annual cycle of the CBNLLJ have not been documented. Also unknown is if there is a diurnal cycle in the low-level winds over the Caribbean and what would control it. Knowing the controls on the CBNLLJ over the calendar year and over the daily timescale is important for predictability and the potential connection of the CBNLLJ to moisture fluxes and precipitation at these timescales.

In summary, even though there is documentation on the existence of a low-level jet over the Caribbean, there are still unknowns about what controls the CBNLLJ and about the influence of such a jet on the regional climate. The Caribbean Sea is a source of moisture to its western and northwestern regions and one potential carrier of such exported moisture is the CBNLLJ. However, the role of the CBNLLJ on the moisture transport to the downwind regions is unknown. Also, the CBNLLJ may be related to the difference in intensity of precipitation between the weaker precipitation in the Caribbean and the stronger precipitation in the northeastern tropical Pacific regions (albeit the presence of warm pools in both regions). That is to say, the role of the CBNLLJ on the regional hydroclimate including the moisture fluxes, the *canícula* and the precipitation needs to be investigated for the CBNLLJ may be an important modulator. In addition, which factors lead to the onset of the CBNLLJ and if the

CBNLLJ has a diurnal cycle merits to be investigated. The existence of a strong diurnal cycle may be important in relation to the diurnal cycle of precipitation.

## 2.2 Other American low-level jets

Better documented are the low level jets (LLJs) of North and South America for which several hypotheses have been developed to explain their existence (Nogues-Paegle and Paegle, 2001). The Great Plains LLJ (GPLLJ), east of the Rocky Mountains, and the South American LLJ, east of the Andes, play an important role in the exchange of atmospheric water vapor from low to mid-latitudes. It is hypothesized that their existence is due to the diurnal oscillation of the boundary layer convergence in the vicinity of the Rockies or Andes (Nogues-Paegle and Paegle, 2001). They have also been related to downwind precipitation and convective activity, especially during the night.

In fact, the GPLLJ shows a diurnal cycle being stronger during the night. The GPLLJ diurnal cycle and its nighttime maxima have been attributed to the day to night reduction of turbulent mixing (Blackadar, 1957), diurnally oscillating buoyancy forces above sloping terrain (Holton, 1967), or combinations of the two effects (Bonner and Paegle, 1970). Wexler (1961) has discussed the blocking influence of the topography. On interannual timescales the GPLLJ seems to be related to droughts and floods in the Great Plains, e.g., the drought episode of 1988 and the flood episode of 1993 (Castro et al, 2001). An important aspect of the GPLLJ is its capacity to transport moisture from remote upwind regions and trigger convective activity downwind.

The maximum of the South American LLJ (SALLJ) is present all year round though it is strongest in austral winter (Berbery and Barros, 2002; Nogues-Paegle et al, 2002). It has been documented that the SALLJ transports water vapor from the Amazon basin to central South America (Berbery and Collini, 2000; Berbery and Barros, 2002). For the SALLJ, several mechanisms have been proposed. Vera et al (2006) summarizes the hypothesized mechanisms as due to: the deflection of the trade wind circulation that crosses the Amazon basin; the topography of the region and dry dynamics; variations in the pressure field in northern Argentina associated with transient westerlies; and propagation of westerly wind bursts from the North Atlantic towards the La Plata Basin through the Amazon basin.

The documentation for the GPLLJ and for the SALLJ is more extensive than the documentation for the CBNLLJ. Hypotheses have been formulated for the GPLLJ existence and the SALLJ existence, but what controls the CBNLLJ and what leads to its formation needs explanation. Indeed, one of the main differences between the continental LLJs (GPLLJ and SALLJ) and the CBNLLJ is that the latter exists over a body of water, the Caribbean Sea. Furthermore, the CBNLLJ has a zonal orientation (whereas the SALLJ and the GPLLJ have a meridional orientation) and it may influence the Caribbean SSTs by coastal upwelling. The paramount role of the LLJs in the hydroclimate of their domain is explicit for the GPLLJ and the SALLJ cases. The CBNLLJ may also play an important role on the regional hydroclimate and needs clarification.



### 2.3 Remote influences on the tropical North Atlantic and Caribbean regions

The tropical North Atlantic is subject to external forcing by the El Niño – Southern Oscillation (ENSO) and the North Atlantic Oscillation (NAO). The Caribbean region is also influenced by large-scale anomalous climate patterns. In general, tropical North Atlantic (TNA) SST has a lag relationship to ENSO (Enfield and Mayer, 1997; Saravanan and Chang, 2000). ENSO winter warming in the equatorial Pacific gives rise to a delayed warming in the northern tropical Atlantic in spring through subsidence associated with anomalous Hadley and Walker circulations (Wang, 2005). During the warm phase of ENSO there is convection, surface convergence, and divergence aloft in the central-eastern Pacific. The Pacific divergence aloft leads to upper convergence over the tropical western Atlantic where the Atlantic Hadley cell has weakened with sinking over the tropical Atlantic and reaching the surface between 10°N and 20°N over the TNA. Relevant to the CBNLLJ would be the effect of ENSO on the North Atlantic High. By influencing the North Atlantic High the TNA gradient of SLP would have a strong influence on the CBNLLJ.

The Caribbean region is also influenced by ENSO. Among the several studies that have documented the influence of the Southern Oscillation (SO) or ENSO on the Caribbean precipitation are Rogers (1988), Chen and Taylor (2002), Giannini (2000) and a scientific note by Magaña (2000).

Rogers (1988) studied the precipitation variability over the Caribbean and tropical Americas associated with the Southern Oscillation. He used data from about 197 stations for a period of about 20 years and analyzed seasonal precipitation anomalies

for the two Southern Oscillation (SO) modes in the tropical Pacific: the high-dry mode (or the atmospheric counterpart to La Nina events) and the low-wet mode (or the atmospheric counterpart to El Niño events). Rogers (1988) finds that during boreal autumn (October-December) and winter (January-March) precipitation is significantly higher for the high-dry mode of the SO at most stations in the eastern Caribbean, Central America and northern South America while for the higher latitudes of the region, i.e., over southern United States, Cuba and Mexico, precipitation is higher during the low-wet SO mode. Two almost opposing seasons are spring (April-June) and summer (July-September) given that, according to Rogers (1988), throughout almost the entire region from the equator to 30°N the precipitation during spring is dominated by the low-wet SO mode while during summer the precipitation is dominated by the high-dry SO mode.

Chen and Taylor (2002) showed that during the early Caribbean rainy season (May-July) the precipitation variability is dominated by a mode with greater loadings in the Caribbean basin south of 20°S. This mode is highly correlated with Niño3 and Niño4 indices several months before such that warm Pacific conditions in winter are correlated to May-July positive rainfall departures in the Caribbean region south of 20°S. This is in agreement with the results of Rogers (1988) whose spring season (April-June) has two months in common with the early Caribbean rainy season (May-July) studied by Chen and Taylor (2002). Giannini et al (2000) also addressed precipitation rates in the earlier part of the rainy season indicating a strong positive relationship between early season Caribbean rainfall and El Niño events that peaked a few months before in winter.

Giannini et al (2000, 2001) discuss the variability of Caribbean and Central American precipitation with respect to regional and large-scale climate anomalies. Giannini et al (2000) performed canonical correlation analyses on land station data of precipitation. For July-August, or midway through the Caribbean rainy season, they identified that associated with less precipitation over much of the Caribbean there is an interbasin pattern of sea level pressure (SLP) with low SLP over the Pacific and high SLP over the Atlantic. Between SST and precipitation, the ENSO mode dominates from July through October with warm eastern Pacific SST associated with negative rainfall anomalies in the Caribbean. Looking for the relation between the SLP interbasin gradient and ENSO they show that the Niño3 index in December-January correlates significantly with the SLP seesaw in the previous July-August such that the relation corresponds to the onset of ENSO events during late summer. The onset of a warm ENSO event is reflected in the Caribbean by a reduction of precipitation during boreal summer.

Magaña (2000), in a concise note without indication of data sources, discuss the precipitation patterns over Mexico, Central America, and the Caribbean related to ENSO warm and cool phases. Magaña (2000) present composites of precipitation during June-September for ENSO warm and cool phases (regardless of onset or decay summers), showing that for El Niño summers there are negative precipitation anomalies over most of Mexico and Central America while for La Nina summers precipitation is normal or higher than normal. Magaña (2000) hypothesizes that the mechanisms that produce the precipitation deficit during El Niño summers include: a southward shift in the ITCZ over the eastern Pacific; enhanced subsidence over

northern Mexico; and a stronger low-level jet over the Caribbean. For La Nina summers Magaña (2000) hypothesizes that precipitation is normal or higher than normal as a result of an ITCZ around 10°N; weaker trade winds over the IAS; and weaker subsidence over northern Mexico. Although Magaña (2000) does not discuss how these mechanisms come about as a result of ENSO warm or cool phases, it is suggested that the Caribbean and Central American region is subject to remote influences and that one of the features by which teleconnections influence the region is the Caribbean Low-Level Jet (CBNLLJ).

In summary, the influence of ENSO on Caribbean and Central America precipitation is characterized by a reduction (increment) of precipitation during the onset of warm (cool) ENSO events during the late rainy season and by an increment (reduction) of precipitation months after the peak of a warm (cool) ENSO event during the early rainy season. One of the mechanisms hypothesized to induce the Caribbean precipitation changes during the onset of ENSO events is the CBNLLJ. However, how the CBNLLJ serves as a medium between ENSO and the precipitation regional to the CBNLLJ is unknown. Hence a greater understanding of the CBNLLJ is important to understand the influence of the Pacific ENSO on the Caribbean and Central American precipitation.

Studies that have documented the influence of ENSO on the CBNLLJ are Mora and Amador (2000) and Amador and Mo (2005). Mora and Amador (2000) discussed the CBNLLJ behavior for Pacific El Niño and La Nina events from composites of the 925 hPa zonal wind for El Niño and La Nina years. Mora and Amador (2000) made the composites based on the period 1982-1997 and identified El Niño events for the

years 1982, 1987, 1991, 1992, 1993, 1994, 1997 and La Nina events for the years 1988, 1989, 1996 (it is not clear if they included 1996 or not in the La Nina composite). They observed that for El Niño events the CBNLLJ intensifies (on the order of about 1 m/s) consistently from 1000 hPa through 850 hPa. For La Nina events the CBNLLJ weakens (about 1.5 m/s) from 1000 hPa through 850 hPa. The composites of the meridional wind anomalies show small values indicating that the zonal wind anomalies play the dominant role on the low-level flow anomalies. When considering SSTs in the Pacific, Amador and Mo (2005) also observe that warm conditions in Pacific are associated with a stronger Intra-Americas LLJ. In general, ENSO influences the CBNLLJ. However, it is unknown how ENSO modulates the CBNLLJ and if ENSO is the sole remote forcing of the CBNLLJ during summer. Understanding the mechanisms by which ENSO relates to the CBNLLJ is important for its potential connection to the precipitation variability in the region, as discussed above.

In addition, ENSO has an influence on Caribbean SSTs, in part, through the triggered anomalies of the low-level winds. Alexander and Scott (2002) used observations and performed model experiments to study the influence of ENSO on air-sea interaction in the north Atlantic, Gulf of Mexico and the Caribbean Sea. They forced an atmospheric GCM with observed SSTs in the tropical Pacific, while over the remainder of the global oceans SSTs were simulated by a mixed layer model. Alexander and Scott (2002) confirmed the observed (thermodynamic) warming in the tropical North Atlantic and cooling in the Gulf of Mexico in the winter-spring after ENSO peaks. Also, they found that during the summer prior to the peak of ENSO

(i.e., the onset of ENSO), latent heat fluxes generate SST anomalies in the Caribbean during August-October. They broke up the bulk formulas for latent heat flux ( $Q_{lh}$ ) and sensible heat flux ( $Q_{sh}$ ) into their time mean and departures from the mean, (e.g.,  $U'\overline{\Delta q}$  and  $\overline{U}\Delta q'$  for  $Q_{lh}$ ), and confirmed that  $U'$  is essential for generating the SST anomalies in the tropics while  $\Delta T'$  and  $\Delta q'$  are more important at mid and high latitudes. The model results showed anomalously cold water extending over the Caribbean and the eastern subtropical Atlantic during September of the onset year (Sep(0)) of a Pacific warm event. The negative SST anomalies during Sep(0) are primarily due to  $Q_{lh}$  anomalies although  $Q_{sw}$  also cools the ocean between 15°N-20°N. The essential  $U'$  and  $Q_{lh}$  anomalies for generating SST anomalies lead to the CBNLLJ role on the connection between ENSO and Caribbean SSTs. The relevance of the CBNLLJ on the ENSO influence on Caribbean SSTs is then implicit through Alexander and Scott (2002) findings.

Wang and Enfield (2001, 2003) studied the Western Hemisphere Warm Pool (WHWP) as the area of the northeastern tropical Pacific, the Intra-Americas Sea and the western tropical North Atlantic (TNA) with SSTs greater than 28.5°C. Wang and Enfield (2001, 2003) defined two indices: an intensity index as the SSTA averaged over the rectangular region of 7-27°N, 110-50°W and an area index as the area enclosed by the 28.5°C isotherm. They found that the Niño3 SSTA index has a correlation of 0.63 with the WHWP SSTA index when the Niño3 index leads by 3 months. From 1950-1999 only 5 of the 9 El Niño events were followed by a large WHWP. Wang et al (2006) also calculated the correlations, but for separate seasons paying particular attention to the Atlantic side of the WHWP, the Atlantic warm pool

(AWP). The correlation between December-February Niño3 SSTAs and the May-July AWP index is 0.60, indicating that in the Caribbean early rainy season, the AWP size has about 35% explained variance from winter Niño3 SSTAs. The correlation between December-February Niño3 SSTAs and August-October AWP index drops and Wang et al (2006) concluded that about two thirds of the AWP variability in August-October appears unrelated to ENSO during the previous winter. They also find that the contemporaneous correlation between August-October Niño3 SSTAs and the August-October AWP index is not significant (and do not provide the correlation coefficient). They concluded that the AWP is more related to the TNA SSTAs than to ENSO.

The studies by Alexander and Scott (2002) and Wang et al (2006) found that ENSO affects Caribbean SSTs. However, while Alexander and Scott (2002) observed that there are opposite SST anomalies between the Caribbean and the equatorial Pacific during the summer onset of Pacific ENSO events, Wang et al 2006 do not observe a significant correlation (or anti-correlation) between Niño3 and the size of the AWP during August-October. The wind and latent heat flux anomalies observed by Alexander and Scott (2002) may reflect changes in the CBNLLJ and may prove the CBNLLJ to be a link between tropical Pacific SSTs and Caribbean SSTs. More studies focused specifically on the CBNLLJ relation to Caribbean SSTs and tropical Pacific SSTs are needed.

#### 2.4 Tropical and North Atlantic relation to Caribbean precipitation

The North Atlantic SST also has variability driven by the North Atlantic Oscillation (NAO; Visbeck et al, 2003). The NAO modulates the strength of the

northeast trades and as a consequence modulates the SST in the subtropical North Atlantic. An index of the NAO is the difference in pressure between the Azores region and the Iceland region (Hurrell et al, 2003). A high NAO index (Azores SLP higher than Iceland SLP) is indicative of strengthened atmospheric Ferrel and Hadley circulations which translate into surface westerly wind anomalies over the North Atlantic and surface easterly wind anomalies over the middle to subtropical Atlantic. Hence, the northeasterly trades are strengthened during positive NAO events which translate into cooler SSTAs over the TNA. The CBNLLJ may also respond to NAO forcing, but it has not been documented.

The NAO and TNA influence on Caribbean precipitation has been studied by Malmgren et al (1998) and Giannini et al (2001), among others. Malmgren et al (1998) studied the ENSO and NAO control of climate on Puerto Rico. Puerto Rico is located in the northeast region of the Caribbean Sea roughly at (18°N, 65°W). Using mean air temperature and precipitation records from five climate stations in Puerto Rico for a record length of almost the entire 20<sup>th</sup> century, Malmgren et al (1998) found that El Niño years are associated with warm air temperatures over the island whereas for La Nina years there are cooler air temperatures. Malmgren et al (1988) also found that the annual rainfall amounts are synchronous with variations of the NAO during winter and are not related to ENSO. That is, during years of a high winter NAO index, annual precipitation in Puerto Rico is lower than average. The lack of relation between equatorial Pacific SSTs and Puerto Rico annual rainfall may be due to the changing relation between seasonal precipitation and ENSO throughout the year. That is, as discussed above, the early summer Caribbean rainy season is



positively correlated with peaks of ENSO a few months before (i.e., winter) while the late summer Caribbean rainy season is negatively correlated with concurrent ENSO conditions.

Giannini et al (2001) extended the analyses of Giannini et al (2000) to consider the NAO. They found that a stronger-than-average North Atlantic High during boreal winter (December-March) leads to cooler tropical North Atlantic (TNA) SSTs which in turn result in negative rainfall anomalies during the following seasons, the rainy seasons. In other words, a positive NAO and its associated stronger northeasterlies lead to cooler SST over the TNA through thermodynamic cooling (Czaja et al, 2002). The cooler SSTs do not trigger convection and result in drier conditions during the summers following positive NAO phases. This anti-correlation is in agreement with the results of Malmgren et al (1998). Hence, while a positive NAO event in winter is associated with drier conditions (less precipitation) over the Caribbean during the summer, the onset of a warm ENSO event is also related to less precipitation over the Caribbean during summer (Giannini et al, 2001). That is, the sequence of positive NAO events during winter and warm ENSO onsets during summer would add up to suppress precipitation over the Caribbean during the summer months. Giannini et al (2001) indicated that from 1979 to 1999 four out of the six warm ENSO events were preceded by positive NAO events the previous winter, resulting in less precipitation over the Caribbean for the summer months.

The influence of the NAO on the CBNLLJ is plausible as the CBNLLJ seems to be the southwestern flank of the North Atlantic High (which is influenced by the

NAO). The relation of the NAO and the CBNLLJ may be significant, but has not been quantified and needs to be studied.

Another oscillation of the North Atlantic that may influence the CBNLLJ is the Atlantic Multidecadal Oscillation (AMO; Enfield et al, 2004; Knight et al, 2006). The AMO is an internal and natural oscillation of the North Atlantic surface temperature that varies on multidecadal timescales. The AMO is quantified as the 10-year smoothed and detrended sea surface temperature anomalies in the North Atlantic from the equator to 70°N (excluding the Mediterranean Sea) as explained in Enfield et al, 2004. Knight et al, 2006 presented evidence that the AMO affects the sea level pressure in the tropical North Atlantic including the Caribbean Sea region. When the AMO is in its positive phase (warm North Atlantic) the pressure in the TNA decreases whereas the precipitation increases (Knight et al, 2006). Through modulation of the pressure in the TNA the AMO may have an influence on the CBNLLJ on multidecadal time scales.

Taylor et al (2002) studied the influences of the tropical Atlantic and Pacific on the rainfall of the Caribbean region partitioned into an early rainy season (May-July) and a late rainy season (August-October). They defined an index of the rainfall of the region by averaging the precipitation over the area 10°N-20°N and 83°W-65°W. The data set used was the monthly gridded (0.5° x 0.5°) analyses of Magaña et al (1999) which is a hybrid of rain gauge, satellite and model (reanalysis) data. Taylor et al (2002) observed an association between greater precipitation over the Caribbean and Central America and a west-east gradient of SST between the equatorial (cool) Pacific and (warm) Atlantic oceanic basins, in particular for the late rainy season

(August-October). A similar relationship between the regional precipitation and a Pacific-Atlantic interbasin SST gradient (and an interbasin SLP gradient) was also observed by Giannini et al (2001). This relationship points to the importance of large-scale climate anomalies on the precipitation variability over the Caribbean and Central America.

Overall, Caribbean precipitation variability during the warm season is related to an inter-basin difference of SLPAs and SSTAs. Stronger summer Caribbean precipitation is concurrent with a warming of the tropical Pacific and a cooling of the tropical North Atlantic. Additionally, there has been evidence that the NAO in boreal spring affects the TNA SSTAs, most likely having an influence on the Caribbean climate. It has been hypothesized (Magaña, 2000) that the remote influence on Caribbean precipitation acts through the modulation of the Caribbean low-level easterlies. A greater understanding of the factors that influence the CBNLLJ would contribute to a greater understanding of the Caribbean climate interactions.

## Chapter 3 : Methodology

This section focuses on the methods used to analyze the seasonal and interannual variability of the easterly LLJ over the Caribbean Sea and its forcings from the regional and larger-scale climate. Our basic strategy was the following. First, the seasonal variability was characterized by taking into account the sea level pressure gradients and the thermal gradients across the Caribbean region. The maximum of the CBNLLJ in February was contrasted with the July maximum. Then, the main factors that regulate the CBNLLJ interannual variation were diagnosed with respect to the spatial and temporal characteristics from our analysis.

The annual variability of the CBNLLJ was studied primarily from the climatology of the base period from 1979 to 2001. In addition, the CBNLLJ anomalies between the periods 1979-2001 and 1958-1978 were contrasted. Special attention was given to the summer months from June to August. The months from June to August are when the summer CBNLLJ is strongest having an onset in June, a peak in July and decay in August. Also, the months of June and August are months when the CBNLLJ shows high variability from year to year. June and July correspond to the early rainy season of the Caribbean and Central America region while August and September correspond to the late rainy season.

### 3.1 The Data

Several data sets are used for this study. The primary sources of atmospheric data used are the North American Regional Reanalysis (NARR; Mesinger et al. 2006) and

the ECMWF 40-year Reanalysis (ERA-40; Uppala et al. 2005). Reanalyses are the result of a complex procedure of running an atmospheric model and using a method for assimilating observations (Kalnay, 2003). The assimilation of observations is paramount given that models have biases in their forecasts or analyses. The NARR, in addition to assimilating the usual type of observations, assimilates precipitation. In the region of the IAS and other oceanic regions, pentad (5-day) precipitation from CMAP (Xie and Arkin, 1997) was assimilated (Mesinger et al. 2006). The pentad precipitation was disaggregated to hourly precipitation using as reference the NCEP/NCAR Reanalysis (Kalnay et al, 1996) hourly precipitation (Mesinger et al. 2006). Other positive attributes of the NARR are the high horizontal resolution (32 km x 32 km) and vertical resolution (25 hPa below 700 hPa), and a temporal resolution of 3 hours.

However, as implied by its name, the NARR only covers the North American continent and adjacent waters with 7°N as its southernmost boundary and does not cover a large part of the nearby tropical Atlantic and Pacific basins. Utilizing global reanalyses is then suitable because of their greater coverage. The ERA-40 global reanalysis is then used to analyze the large-scale climate connections. Also, the NCEP/NCAR Reanalysis (Kalnay et al. 1996) irrotational and rotational components of the 925-hPa and 250-hPa wind are analyzed. The Comprehensive Ocean-Atmosphere Data Set (COADS; Slutz et al, 1985) was used to corroborate the zonal wind statistics. COADS provides surface wind data obtained from surface marine ship reports.

Precipitation and sea surface temperature (SST) data are also analyzed. The Global Precipitation Climatology Project (GPCP; Adler et al. 2003) provides monthly precipitation with  $2.5^{\circ} \times 2.5^{\circ}$  spatial resolution covering the period since 1979 with a greater spatial coverage than the NARR. The water temperature analysis relied on the NOAA Optimum Interpolation SST (OISST)  $1^{\circ} \times 1^{\circ}$  data set (Reynolds et al. 2002) for the 1982-2001 climatology and on the NOAA Extended Reconstructed SST (ERSST)  $2^{\circ} \times 2^{\circ}$  data set (Smith and Reynolds, 2004) for regression analyses (since the latter has a longer time span).

Several climate indices were used to study the relations of the CBNLLJ with teleconnection patterns and remote influences. Climate indices provide information of a particular climate phenomenon summarized into a single time series suitable for statistical analyses.

The CBNLLJ behavior is summarized as a climate index. As observed from Fig. 2.1, over the Caribbean Sea, the meridional component of the wind is very small compared to the zonal component of the wind. Because of this, the focus of this CBNLLJ study is on the zonal component of the wind. The zonal flow over the Caribbean has a maximum at 925 hPa throughout the year concentrated over the area from  $12^{\circ}\text{N}$  to  $17^{\circ}\text{N}$  and from  $70^{\circ}\text{W}$  to  $80^{\circ}\text{W}$ . The highest year-to-year variability of the 925-hPa zonal wind occurs from June to September and is collocated with the region of the zonal wind maximum. This lends the CBNLLJ to be summarized as an index of the zonal wind at 925 hPa averaged from  $12^{\circ}\text{N}$  to  $17^{\circ}\text{N}$  and from  $70^{\circ}\text{W}$  to  $80^{\circ}\text{W}$ . The CBNLLJ index was calculated from reanalyses data.

Other climate indices are used to study the relations of the CBNLLJ with teleconnection patterns and remote influences. Among the other indices that were used to quantify correlations are the Niño3.4 SST anomaly (SSTA) index, the North Atlantic Oscillation (NAO) index and the Atlantic Multidecadal Oscillation (AMO) index (Enfield et al, 2001). The AMO index was obtained from the NOAA Climate Diagnostic Center website ([www.cdc.noaa.gov/ClimateIndices/](http://www.cdc.noaa.gov/ClimateIndices/)). The AMO index was calculated by computing the area weighted average over the North Atlantic, from the equator to 70°N, detrended the time series and smooth it with a 121-month smoother. The data used were Kaplan SST dataset (5x5) (Kaplan et al. 1998). The NAO index was calculated by NOAA's Climate Prediction Center by applying Rotated Principal Component Analysis (Barnston and Livezey, 1987) to monthly mean standardized 500-mb height anomalies in the region 20°N-90°N. The Niño3.4 index is the SSTA averaged for the area (5°N-5°S; 170°W-120°W). Tahiti SLP station data was provided by the IRI Data Library.

### 3.2 Hypotheses and Approach

#### 3.2.1 Seasonal Variability

By having the Bermuda High or the North Atlantic subtropical anticyclone to its northeast, the Caribbean region is in the southwestern flank of the Bermuda High domain. Such an anticyclone would influence the climatology of the CBNLLJ by the pressure gradients formed and its variability throughout the year. Additionally, the land to the south of the Caribbean region would be influencing the thermal gradients. To the south of the Caribbean Sea the differential heating between land and sea

corresponds to a southward gradient of air temperature which is related to the thermal wind by:

$$\frac{\partial u_g}{\partial p} = \frac{R}{fp} \left( \frac{\partial T}{\partial y} \right)_p,$$

where  $u_g$  is the geostrophic wind,  $p$  is pressure,  $T$  is temperature,  $R$  is the gas constant for dry air and  $f$  is the Coriolis parameter (Holton, 1992). Essentially, the thermal wind is the vector difference between the geostrophic winds at two levels. Hence, a vertical shear of the zonal flow of the lower troposphere should be balanced by a meridional gradient of air temperature. The CBNLLJ was diagnosed within the context of the thermal wind relation.

*Hypothesis A:* The CBNLLJ seasonal peaks are due to a combination of

intensification of the northward sea level pressure gradient and a southward thermal wind.

The following approach was used for the results presented in Chapter 4. The approach was based on the use of climatological maps of assorted variables. The monthly climatology from 1979 to 2001 was quantified (except for OISST which was from 1982 to 2001). First, I analyzed the seasonal cycle of the zonal component of the Caribbean wind in the vertical to determine the level of strongest winds. Then, I focused on a comparison between the CBNLLJ summer peak in July and the winter peak in February by analyzing vertical cross-sections of the zonal wind and the air temperature. The climatology of the CBNLLJ and of the region was analyzed in terms of the zonal wind, sea level pressure (SLP), 925-hPa wind vector, zonal geostrophic wind, air temperature, zonal thermal wind and moisture fluxes. As



further summer analyses, the summer intensification of the CBNLLJ was analyzed from the difference of the May and June monthly climatologies.

The climatological analysis of the hydroclimate was based on factors related to the June-July spatial and temporal minimum of precipitation in the Caribbean, the Caribbean mid-summer drought. Inherent to the precipitation of a region is the moisture flux. The atmospheric branch of the hydrological cycle (Peixoto and Oort, 1992) is given by:

$$\text{div}Q = E - P ,$$

where  $Q$  is the vertically integrated moisture flux,  $E$  is evaporation and  $P$  is precipitation. The vertically integrated atmospheric moisture flux vector is given by:

$$Q = \int_{top}^{sfc} qV \frac{dp}{g} ,$$

where  $q$  is the specific humidity,  $V$  is the vector wind velocity,  $p$  is pressure,  $g$  is gravity,  $sfc$  is the surface and  $top$  is the top of the atmosphere.

To diagnose the diurnal cycle of the CBNLLJ, 3-hourly data was used. Indeed, Mestas-Nuñez et al (2005) indicated that to resolve a diurnal cycle in the Intra-Americas Sea region, higher than 6-hourly temporal resolution is needed (Mestas-Nuñez et al, 2005). Since the NARR provides 3-hourly data it is apt to resolve a diurnal cycle and was used to study the diurnal cycle of the CBNLLJ. The months when the CBNLLJ peaks are July and February and the diurnal variability during these months was analyzed with 3-hourly data.

### 3.2.2 Interannual Variability

To study the variability of the CBNLLJ and its associated climate interactions a suite of statistical techniques were used. The approach was to investigate the interactions using statistical techniques such as correlation and regression. For the interannual variability component I quantified the monthly anomalies for the base period 1958-2001.

*Hypothesis B:* The interannual variability of the CBNLLJ during boreal summer is due, in part, to changes of the Caribbean meridional sea level pressure gradient that in turn affect the magnitude of the zonal winds at 925mb. The interannual variability of these gradients is influenced by the subsidence in the nearby tropical north Atlantic, and changes in the North Atlantic subtropical high.

The northward SLP gradient over the Caribbean is a result of the large-scale climate dynamics that control the subtropical North Atlantic High and other climatological patterns of SLP. Changes in the subtropical North Atlantic High, for example, would translate into changes in the SLP gradients of the Caribbean region and hence affect the intensity of the CBNLLJ. In addition to the NAO, the El Niño - Southern Oscillation (ENSO) may also influence the strength of the CBNLLJ. It is known that when there is a warm Pacific El Niño event, the warm atmospheric anomalies are propagated throughout the tropical troposphere, including that above the Caribbean Sea (Chiang and Sobel, 2002). Also, the sinking and rising branches of

the tropical atmospheric circulation in the tropical North Atlantic change due to ENSO (Wang, 2005).

The following approach was used for the results presented in Chapter 5. I identified the mechanisms of remote forcing of the CBNLLJ by atmospheric and oceanic modes of variability, such as the El Niño-Southern Oscillation. To study the interannual variability of the CBNLLJ, the techniques of correlation and regression were applied to the CBNLLJ index and several atmospheric and oceanic variables and indices with the greater goal of understanding the interactions of the CBNLLJ to the regional and global climate at various leads and lags. Some of the variables that were studied are: zonal wind, meridional wind, sea level pressure (SLP), streamfunction and velocity potential at 925 hPa and 250 hPa, divergent (irrotational) and rotational component of the wind at 925 hPa and 250 hPa, vertical velocity, and sea surface temperature (SST).

Then, the changes in the CBNLLJ were analyzed. Two main approaches were used to analyze the changes in the CBNLLJ. One approach was to study separately the periods 1958-1978 and 1979-2001 by analyzing the changes in the pressure and SST related to the CBNLLJ. The division of the periods in 1978-1979 was based on the advent of satellite-based observations mostly after 1978. Also, the NARR dataset (and other datasets) are available starting from 1979. In fact, a cautionary note should be stated, and it is that the ingestion of satellite-based data may have introduced a bias in the statistics of any of the climate variables. In any case, the difference in the number of years: 21 years from 1958-1978 and 23 years from 1979-2001 is considered for the statistical significance level for each period.

Also, standard deviation of the CBNLLJ index for each of the summer months was calculated by using a sliding window of 21 years to observe the time-dependent changes of the CBNLLJ interannual variability. For example, the standard deviation of the July CBNLLJ monthly anomalies was calculated for the first 21 July anomalies of the record, centered on 1968. The computation was repeated after shifting one value (and being centered on 1969). This was done repeatedly until reaching the 21-year period centered on the year 1991. Notice that a 21-year running mean was not applied, but rather a 21-year running standard deviation. Changes in the standard deviation would be obtained from changes in the frequency or amplitude of the anomalies. Another aspect to consider is that a 21-year running technique will smooth any abrupt changes (such a step function) in the values. Similarly, a 21-year running correlation between SLP (SST) indices in the Caribbean and SLP (SST) indices in the Pacific were computed to determine if the relation between the two basins has changed and if the changes favor more extreme events of the CBNLLJ.

## Chapter 4 : Climatology

### 4.1 Introduction

Although no single definition applies to all LLJs in the global atmosphere, there are a few characteristics that serve to identify an atmospheric LLJ as discussed by Stensrud (1996). The principal criterion is the existence of a maximum in wind speed in a contained area in the lower levels (below 700 hPa) of the atmosphere, i.e., a narrow band of strong winds. The vertical structure of the wind should be one with vertical shear, i.e., a wind vertical profile with weaker winds at the bottom, a maximum in wind speed above and a decrease of wind speed at higher levels. Another criterion is a horizontal wind structure with horizontal shear, i.e., weaker winds at the edges of the jet. These criteria are met by the LLJ in the Caribbean as is demonstrated in this chapter.

A similarity between the CBNLLJ and the GPLLJ and SALLJ is that they flow along mountains. The GPLLJ flows along the eastern side of the Sierra Madre and the Rocky Mountains of North America while the SALLJ flows along the eastern side of the Andes of South America. The Caribbean Sea, over which the CBNLLJ flows, is bounded to the south by the northern coast of South America which has mountains higher than one kilometer. The GPLLJ and the SALLJ have been observed to be influenced by the horizontal temperature gradients due to the topography of their domain (Holton, 1967). The potential of a similar influence from the mountains of northern South America on the CBNLLJ is presented in this chapter.

Other LLJs, such as the Great Plains LLJ and the South American LLJ, have been shown to be important for their potential to transport moisture from remote upwind regions to downwind regions (Blackadar, 1957; Bonner and Paegle, 1970; Berbery and Barros, 2002; Berbery et al. 1996). In this study the moisture fluxes are quantified over the Caribbean Sea from the North American Regional Reanalysis. The relation of the CBNLLJ with the regional hydroclimate is discussed in this chapter.

A purpose of this chapter is, therefore, to identify the mechanisms of the CBNLLJ formation from climatological fields. Also, it aims to identify the CBNLLJ's relation to the regional and large-scale climate (and hydroclimate) during boreal summer. Specific questions that will be addressed: What regional conditions determine the vertical and horizontal structure of the CBNLLJ during its peaks? What large-scale conditions determine the seasonal variability of the CBNLLJ? How is the CBNLLJ related to the moisture fluxes and to the precipitation over the Caribbean Sea?

The presentation of this chapter is as follows. In the following section a discussion of the seasonal and diurnal cycles of the Caribbean zonal winds is presented. This is followed by a characterization of the horizontal and vertical structures of the CBNLLJ. The CBNLLJ is further discussed with respect to the moisture flux structure and seasonal cycle. The basic features of the Caribbean easterly wind relative to the regional mechanisms and factors at play during boreal summer are addressed by discussing the larger-scale seasonal changes that induce the onset of the summer CBNLLJ and the Caribbean summer minimum in precipitation.

## 4.2 The Caribbean low-level jet

### 4.2.1 Seasonal and diurnal variability

The Caribbean wind is predominantly zonal with an easterly direction year round. Figure 4.1 presents the 925-hPa wind vector and speed for February and July (which are the level and months of maximum intensity of the wind). The region of the maximum easterly winds is the central Caribbean Sea between 12°N-16°N and 71°W-76°W. Figure 4.2 presents the vertical profile of the zonal wind averaged in the indicated region of maximum winds. Over the Caribbean Sea the maximum zonal winds are at about 925 hPa (Fig. 4.2) in both the NARR and the ERA-40. At this level, the zonal Caribbean winds fluctuate in strength throughout the year being stronger in July and February and weaker in October and May, indicative of a semi-annual cycle (Fig. 4.2). The seasonal cycle is not sensitive to a bigger area average (e.g., from 12-17°N and 70-80°W) determined by the interannual standard deviation and which will be used for the interannual analyses in Chapter 5.

The July peak of the CBNLLJ is the main peak with winds greater than 13 m/s. In the NARR the July peak is stronger than the February peak by ~1 m/s while in ERA-40 the July peak is stronger than the February peak by ~2 m/s. The main minimum is in October with winds as low as 8.5 m/s. The Caribbean zonal winds from the NARR and the ERA-40 have a similar cycle throughout the year (Fig. 4.2). However, the Caribbean zonal winds of ERA-40 are stronger than the Caribbean zonal winds of NARR throughout the calendar months. Albeit the differences, both reanalyses show the CBNLLJ structure. The LLJ structure will be discussed in the

following section relying mostly on NARR which has higher resolution (than ERA-40) in the horizontal and vertical dimensions and in time.

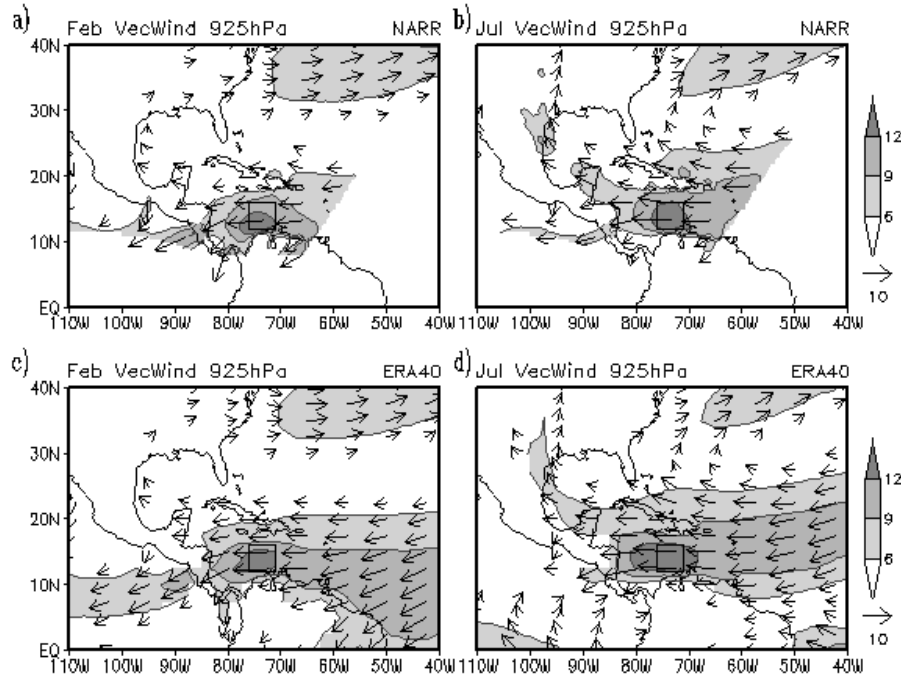


**Figure 4.1.** February (left) and July (right) climatology of 925-hPa winds from the NARR (top) and the ERA-40 (bottom). The base period is from 1979 to 2001. The reference arrow is 10 m/s. The shadings correspond to the magnitude of the vectors in m/s. Vectors with speed less than 3 m/s are not shown. The limits of the NARR domain are observed in the bottom left and bottom right corners of its plots. The rectangle delineates the area of the maximum wind speed from 12°N to 16°N and from 71°W to 76°W.

The variability of the 925-hPa zonal wind throughout the day is characterized by a semi-diurnal cycle in July and February. Figure 4.3 presents the July and February 3-hourly climatology of the zonal wind at 13°N and 74°W, a location of maximum winds in both July and February. At this location the maximum easterly winds in the vertical are at the 925-hPa level. In months, July and February, the 925-hPa easterly wind peaks at 3Z (11PM local time) and 12Z (8AM) with average winds of 15.1 m/s in July and 14.4 m/s in February. These two maxima (at 3Z and 12Z) are divided by



a relative minimum that extends from 6Z (2AM) to 9Z (5AM). The absolute minimum is at 21Z (5PM) with an easterly wind of 12.5 m/s in July and in February. From the afternoon minimum at 21Z (5PM) to the midnight maximum at 3Z (11PM), the easterly wind strengthens 2.7 m/s in July and 1.5 m/s in February. From the morning maximum at 12Z (8AM) to the afternoon minimum at 21Z (5PM) the easterly wind weakens 2.5 m/s in July and 1.7 m/s in February. In both months, the 3Z (11PM) maximum is  $\sim 1.2$  times the 21Z (5PM) minimum. The variability throughout the day, as given by the standard deviation of the 925-hPa zonal wind, is 0.9 m/s in July and 0.6 m/s in February and represents a semi-diurnal variability.

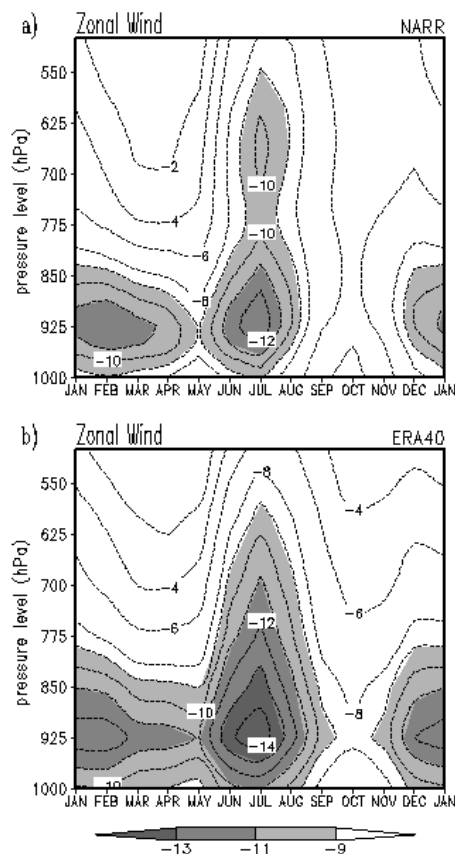


**Figure 4.2. Vertical profile of the zonal wind (m/s) averaged for the column 71°W-76°W and 12°N-16°N from the NARR (top) and the ERA-40 (bottom) for the calendar months. Negative indicates easterly.**

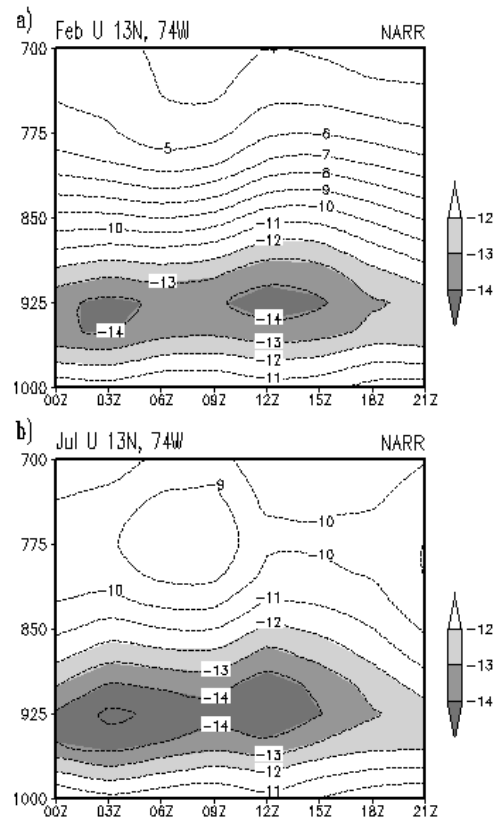


**Figure 4.3. Pressure-time plot of the February (a) and July (b) diurnal cycle of the zonal wind (m/s) at 13°N and 74°W from the NARR.**

#### 4.2.2 Horizontal and vertical structure

In July and February, the CBNLLJ is a regional amplification of the tropical North Atlantic easterly winds. These easterlies are associated with an anticyclone (the Bermuda High) over the subtropical North Atlantic (Fig. 4.4). After flowing over the Lesser Antilles (at about 61°W) the tropical North Atlantic easterlies strengthen becoming strongest over the central Caribbean Sea between 71°W and 76°W and between 12°N and 16°N (Fig. 4.1). In general, the central Caribbean maximum of easterly winds is bounded to the south by the mountains of northern

South America and to the north by the Greater Antilles (at about 19°N). The Caribbean Sea is like a valley bounded to the north and south by mountains higher than 1 km (Fig. 4.5). In both the NARR and the ERA-40 the wind speed reaches values greater than 12 m/s in July and February between 13°N and 15°N (Fig. 4.1). The principal contributor to the wind speed in this region is the zonal component of the wind. There are weaker winds over the northernmost and southernmost Caribbean regions providing the easterly flow a horizontal jet structure with horizontal shear.

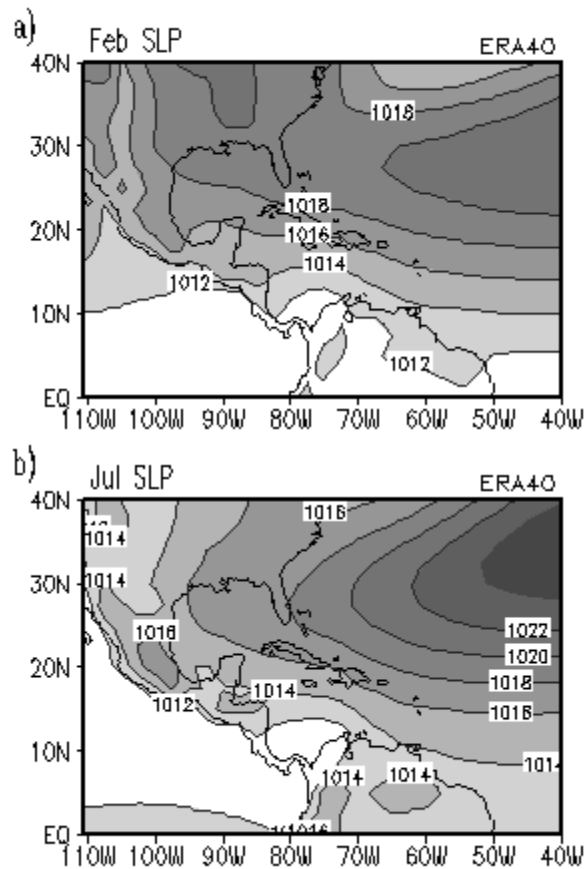


**Figure 4.4. February (a) and July (b) climatology of sea level pressure (hPa) from the ERA-40.**

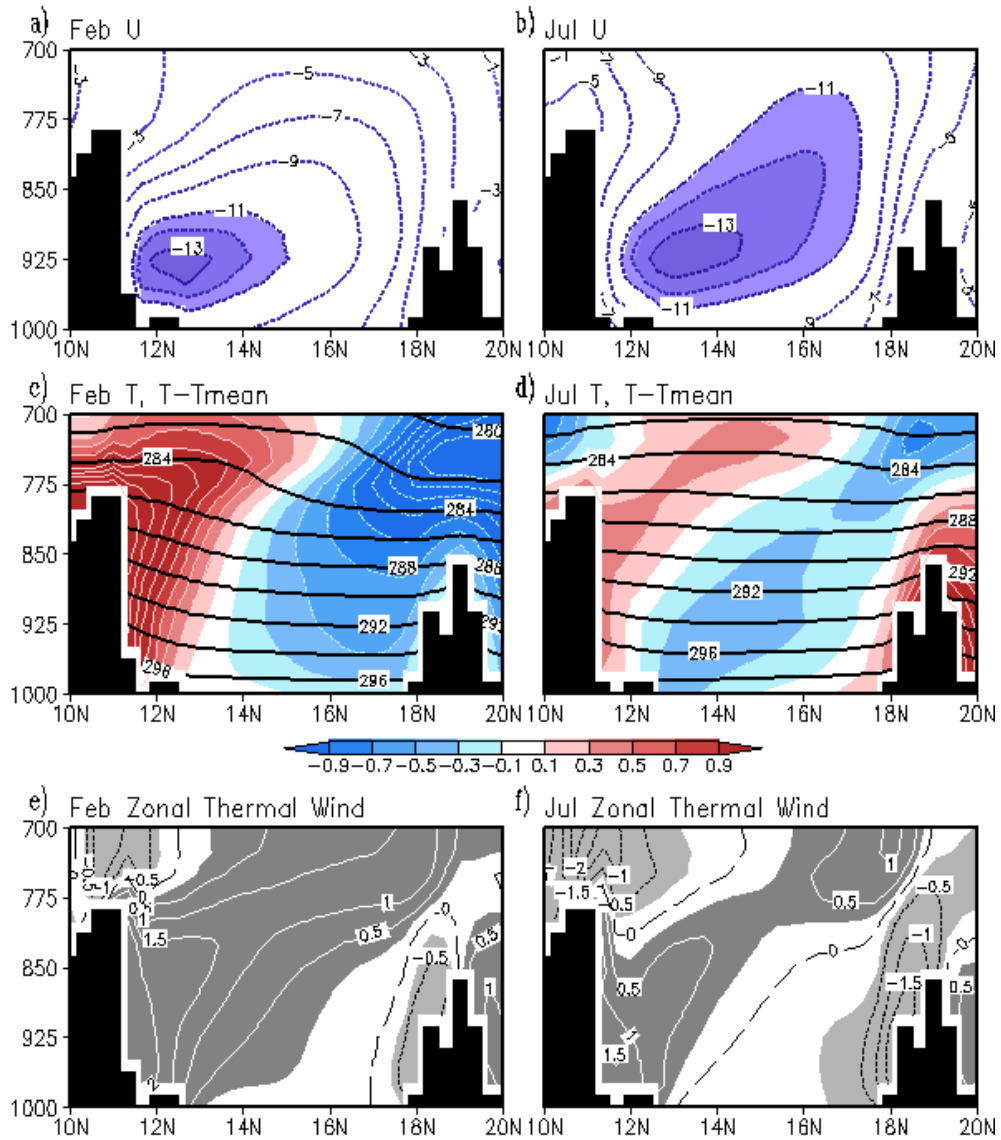


**Figure 4.5.** Pressure-latitude cross-section of February (left) and July (right) zonal total wind, temperature and thermal wind averaged from 71°W to 76°W from NARR. Top panels: Zonal component of the wind (m/s). Negative indicates easterly. Middle panels: Temperature (K, dark contours) and the departure from the meridional (11°N-to-19°N) mean of temperature (K, shadings). Bottom panels: Zonal thermal wind (m/s). Thermal wind values greater than 0.25 (solid contours) are shaded in dark gray while values less than -0.25 (dashed contours) are shaded in light gray. The mountains of South America are observed at 11°N while the mountains of the Greater Antilles are observed at 19°N.

Once the CBNLLJ reaches the western region of the Caribbean Sea the easterly flow bifurcates (divides into two branches) to the northwest (a southeasterly branch) and to the southwest (a northeasterly branch). At the western boundary of the Caribbean Sea the easterlies encounter the mountains of Central America and the speed decreases except through the valleys of Lake Nicaragua ( $12^{\circ}\text{N}$ ,  $85^{\circ}\text{W}$ ) and Panama ( $8^{\circ}\text{N}$ ,  $80^{\circ}\text{W}$ ). As observed from Fig. 4.1, the northeasterly branch of the bifurcation is stronger in February than in July and extends to the northeastern tropical Pacific as the Papagayo Jet and the Panama Jet (Xie et al. 2005). The southeasterly branch of the bifurcation flows over the Yucatan channel and over the Yucatan peninsula into the Gulf of Mexico (Fig. 4.1). This southeasterly branch is stronger in July than in February. The southeasterly branch joins the southerly flow into the gulf states of USA and the Great Plains Low-Level Jet.

The vertical structure of the July and February Caribbean zonal winds with vertical shear throughout the lower levels resembles the structure of a LLJ. Figures 4.5a and 4.5b show the pressure-latitude cross-section of the zonal wind averaged from  $71^{\circ}\text{W}$  to  $76^{\circ}\text{W}$  in July and February from the NARR. In the vertical, the July and February Caribbean easterlies are maximum at the 925-hPa level and weaker below and above that level. In NARR the maximum is concentrated at  $13^{\circ}\text{N}$ , closer to the mountains of northern South America. There are weaker winds to the north and south of the  $13^{\circ}\text{N}$ -maximum with a difference of 6 m/s. This vertical structure with vertical and horizontal wind shear is akin to a low-level jet structure.

Over the Caribbean the geostrophic wind, calculated from the horizontal gradient of geopotential heights, compares well to the total wind between 700 hPa and 950

hPa (figure not presented). Over the central Caribbean ( $14^{\circ}\text{N}$ - $16^{\circ}\text{N}$ ) between the 800-hPa and the 925-hPa levels the geostrophic zonal wind is less than 5% different from the total zonal wind in July and February. However, below 975 hPa the easterly total wind is weaker than the easterly geostrophic wind and their difference is greater than 25% as the surface is approached. The difference below 950 hPa is indicative of the frictional effects of the planetary boundary layer. The vertical effect of friction manifests as a vertical profile with vertical shear, i.e., weaker winds closer to the surface and stronger winds above 925 hPa.

The meridional gradients of temperature in the Caribbean indicate a baroclinic structure close to the mountains of northern South America. Figures 4.5c and 4.5d present the pressure-latitude cross-section of the temperature and the departure from the meridional ( $11^{\circ}\text{N}$ -to- $19^{\circ}\text{N}$ ) mean of temperature in February and July. In both months, throughout the vertical range of the mountains of northern South America, the temperature increases southward from the central Caribbean ( $14$ - $15^{\circ}\text{N}$ ) towards the mountains (Figs. 4.5c and 4.5d). Figures 4.5e and 4.5f present the zonal thermal wind averaged from  $71^{\circ}\text{W}$  to  $76^{\circ}\text{W}$ . The zonal thermal wind, a measure of the vertical shear of the zonal geostrophic wind, was calculated from the temperature change in the meridional direction according to eq. 3.32 of Holton (1992). It is observed that the thermal wind is positive and strongest in the southern part of the Caribbean Sea below the 775-hPa level (Figs. 4.5e and 4.5f). Where the thermal wind is positive, the easterly geostrophic wind increases with pressure (i.e., the zonal geostrophic wind becomes more negative as the surface is approached). The southward gradient of temperature and the stronger thermal wind represent a

baroclinic structure favorable for a stronger easterly wind over the southern part of the Caribbean. Hence, the influence of the warming of the highlands of northern South America on the southward temperature gradient represents a regional influence on the intensification of the CBNLLJ.

However, in the northern part of the Caribbean the influence of the highlands (the Greater Antilles) weaken the easterly winds below 800-hPa. In July (Figs. 4.5d and 4.5f), the temperature close to the southern slope of the Greater Antilles is warmer than over the central Caribbean. In this case, the northward gradient of temperature counteracts the pressure gradient by weakening the easterly wind. This northward gradient of temperature over the northern part of the Caribbean is strongest in the summer months as the Greater Antilles and the Caribbean waters are warmed by the seasonal march of the sun (not presented). It may be this competing effect between the southward and the northward temperature gradients induced by the mountains to the south and to the north, which provides the CBNLLJ a slanted orientation in the vertical with a maximum over the southern Caribbean between 900 hPa and 950 hPa (Fig. 4.5b).

#### 4.2.3 Caribbean moisture flux structure and seasonal cycle

The zonal moisture flux across the central Caribbean (averaged from 71°W to 76°W) is presented in Fig. 4.6 for February (panel a) and July (panel b). The zonal moisture flux is calculated by multiplying the zonal component of the wind by the specific humidity. The region of the maximum easterly moisture flux is lower in the atmosphere than the region of the maximum easterly winds because the specific

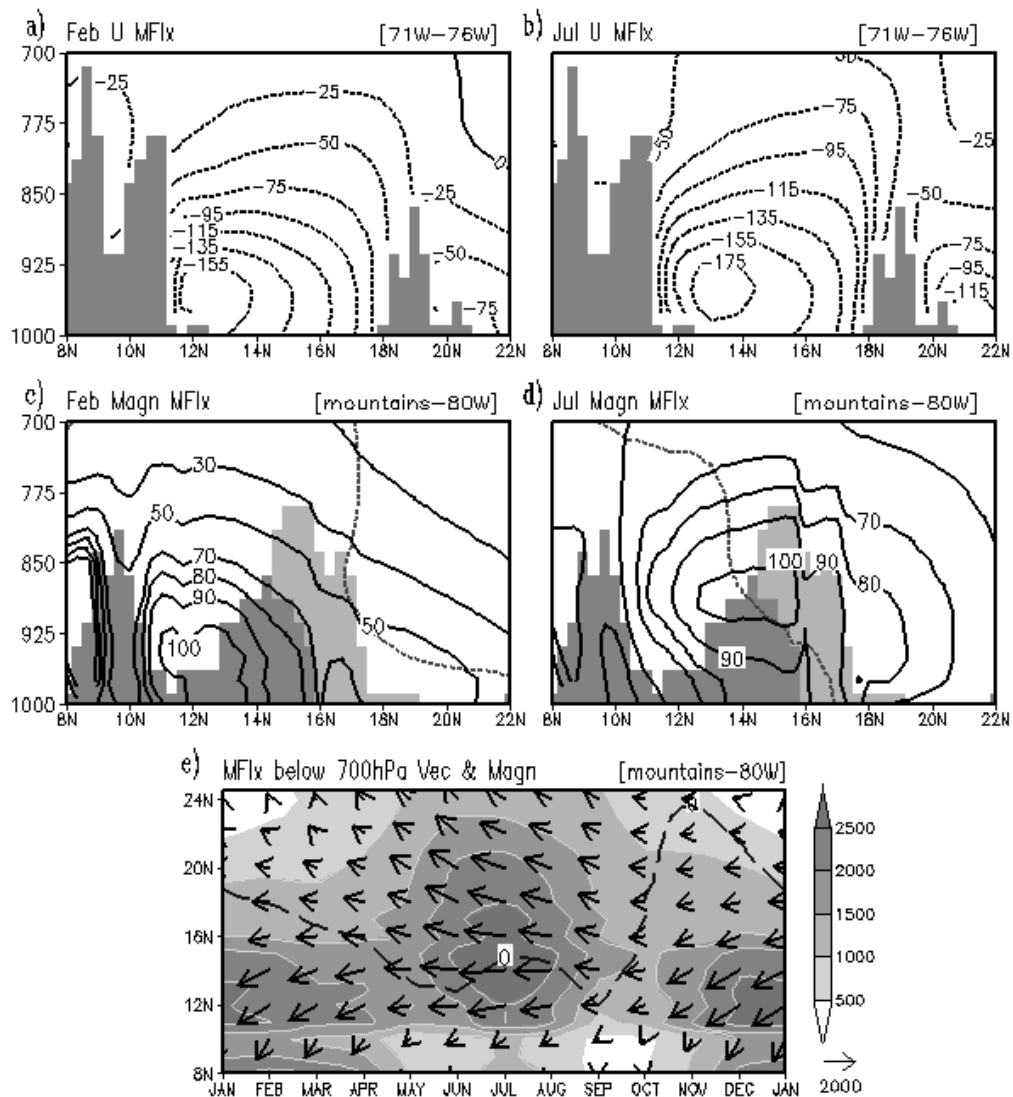


**Figure 4.6.** Pressure-latitude cross-sections and seasonal cycle of moisture flux from NARR. Top panels: Zonal moisture flux ( $\text{m/s}\cdot\text{g/kg}$ ) averaged from  $71^\circ\text{W}$  to  $76^\circ\text{W}$  for (a) February and (b) July. The mountains of northern South America and the Greater Antilles are shaded. Middle panels: Magnitude of the moisture flux vector ( $\text{m/s}\cdot\text{g/kg}$ ) averaged from  $80^\circ\text{W}$  to the eastern side of the mountains of Central America or to  $93^\circ\text{W}$  for (c) February and (d) July. The dashed line indicates where the meridional moisture flux is zero. The mountains of Central America are shaded in the background. Mountains shaded lighter are to the west of  $88^\circ\text{W}$ . Bottom panel: Annual cycle of the moisture flux ( $\text{m/s}\cdot\text{g/kg}$ ) averaged from  $80^\circ\text{W}$  to the eastern side of the mountains of Central America or to  $93^\circ\text{W}$  and vertically integrated from 700 hPa to 1000 hPa. The moisture flux vector is represented by arrows and the magnitude is shaded. The dashed line is the zero-meridional moisture flux.



humidity is larger at lower levels. Nonetheless, the zonal moisture flux also has a jet-like structure with greater easterly moisture flux centered at 13°N and weaker values to the south and to the north. The July easterly moisture flux has a maximum of 186 g/kg·m/s centered at 13°N and 950 hPa. In February the maximum of the easterly moisture flux is of 171 g/kg·m/s centered at 12.6°N and 950 hPa. These maxima are close in magnitude and are in the southern Caribbean closer to the mountains of northern South America. However, during July the easterly moisture flux below 700 hPa and between 11°N and 19°N (i.e., between the mountains) is greater than in February ( $3.5 \times 10^6$  kg/m in July and  $2.5 \times 10^6$  kg/m in February). The difference in zonal moisture flux between February and July is due to both the greater specific humidity (not presented) and the stronger easterlies below 800 hPa in July than in February.

As indicated before, the flow over the western Caribbean bifurcates into a southeasterly branch and a northeasterly branch. Figures 4.6c and 4.6d present the magnitude of the moisture flux vector averaged from 80°W to the eastern side of the mountains of Central America. The moisture fluxes west of where the terrain reaches the 975-hPa level were not included in this calculation of the zonal average from the NARR. Given this criterion, for example, the moisture fluxes over the Yucatan peninsula were included because of the low-altitude terrain, but those over the highlands of Costa Rica and to the west were not included in the zonal average from 80°W to 93°W. Figure 4.6e presents the seasonal cycle of the moisture flux vertically integrated from 700 hPa to the surface. Throughout the year in the western Caribbean

region the zonal direction of the moisture fluxes (and of the wind) is easterly and the meridional direction is northerly over the southern part and southerly over the northern part. The split point (the bifurcation latitude) of the moisture flux in the western Caribbean is defined to be where the meridional moisture flux is zero (the dashed line in Figs. 4.6c-e) and is used to determine when and where the moisture fluxes from the central Caribbean contribute the most to the moisture budget of the Gulf of Mexico.

The annual cycle of the moisture fluxes over the western Caribbean is similar to the annual cycle of the central CBNLLJ with peaks in winter and July and minima in May and October (Figs. 4.6e and 4.7b). In July the southeasterly moisture flux into the Gulf of Mexico is twice as much as in February (Figs. 4.6c-e). Also, the bifurcation of the flow over the western Caribbean lies more to the south in July than in February. This indicates a greater fetch of moisture from the Caribbean into the Gulf of Mexico in boreal summer. Below the 700-hPa level, about 2000 g/kg·m/s flow northwestward in July (Fig. 4.6e) with greater amounts between 850 hPa and 975 hPa (Fig. 4.6d). The southeasterly and northeasterly branches have almost the same magnitude in July (Fig. 4.6d). In February most of the moisture flux over the western Caribbean is northeasterly with greater concentration below 900 hPa (Fig. 4.6c). The winter peak of the CBNLLJ has greater influence on the moisture fluxes on the southern half of Central America while the summer peak of the CBNLLJ has greater influence on the northern half of Central America and the Gulf of Mexico.

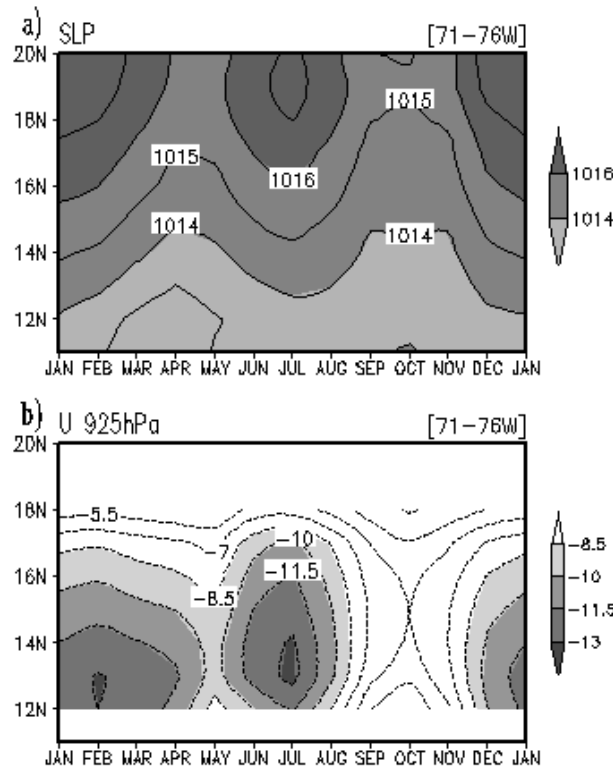


**Figure 4.7. Annual cycle of the 71°-76°W zonal average of (a) sea level pressure (hPa, contour interval of 2 hPa) and (b) 925-hPa zonal wind (m/s, contour interval of 1.5 m/s) from NARR. The Greater Antilles are at about 19°N and South America at 11°N.**

### 4.3 Summer climate and the Caribbean LLJ

#### 4.3.1 Onsets of the Caribbean LLJ

The July and February peaks of the CBNLLJ are coincident with strong northward gradients of SLP across the Caribbean Sea. The southwestern fringes of the Bermuda High (i.e., the subtropical North Atlantic (SNA) anticyclone) extend to the region of the Greater Antilles (Fig. 4.4). Figure 4.7 shows the SLP across the Caribbean region averaged zonally from 71°W to 76°W. Throughout the year, the pressure in the southern Caribbean is less than to the north (a northward pressure

gradient). As observed from Fig. 4.7, over the southern Caribbean Sea, at 12°N, the pressure does not vary throughout the year as much as to the north, at 18°N, where the 1016-hPa isobar is seen to intrude in January and July and retract in May and October. During January and July (May and October) the anticyclone over the SNA has strengthened (weakened) and the SLP northward gradient across the Caribbean strengthens (weakens). The semi-annual cycle of the northward SLP gradient is in phase with the semi-annual cycle of the zonal wind across the Caribbean Sea.

The changes in SLP in boreal winter over the SNA are coherent with subsidence over the SNA from the Atlantic Hadley cell. During boreal winter there is a cross-equatorial overturning circulation with rising motion over the southern subtropics and sinking motion over the northern subtropics. This interhemispheric (southern-to-northern hemisphere) Atlantic Hadley cell is related to the boreal winter (December-February) anticyclone over the SNA. That is to say, the formation during winter of the continental high over North America intensifies the meridional pressure gradient across the Caribbean.

On the other hand, the summer subtropical anticyclone over the SNA has been explained as a remote response to the Asian summer monsoon heating (Chen et al. 2001) and the monsoonal heating over North America (Rodwell and Hoskins, 2001) amplified by air-sea interactions (Seager et al. 2003). As Rodwell and Hoskins (2001) indicate, the effect of the Asian monsoon heating is amplified by the interaction with the mid-latitude westerlies producing adiabatic (and diabatically-enhanced) descent and longwave cooling to the east (Rodwell and Hoskins, 2001) of the anticyclone. To its west, monsoonal heating over land triggers a Kelvin wave

response forming the equatorward flank of the anticyclone (Rodwell and Hoskins, 2001) and contributes to the zonal asymmetries of sea surface temperature (across the basin) that amplify the subtropical anticyclone (Seager et al. 2003).

The Caribbean zonal winds strengthen by  $\sim 3$  m/s from May to June representing the onset of the summer CBNLLJ. For further discussion of the intensification of the Caribbean easterly wind I show the changes from May to June of the rotational wind and its divergence, and the irrotational wind and its vorticity at 925 hPa and 250 hPa in Fig. 4.8. To facilitate the discussion a line from  $20^{\circ}\text{N}$ ,  $70^{\circ}\text{W}$  to  $30^{\circ}\text{N}$ ,  $50^{\circ}\text{W}$  serves as a guide for comparisons. As the Central American monsoon intensifies from May to June the region of upper-level divergence shifts from the northeast of South America to Central America (Fig. 4.8a). The upper-level irrotational outflow from the Central American region connects to a region of upper-level convergence northeast of the Greater Antilles. The region northeast of the Greater Antilles also shows an increase of mid-tropospheric subsidence (not presented), of lower-level divergence (Fig. 4.8c) and of lower-level anticyclonic relative vorticity (Fig. 4.8d). In the tropical Atlantic at around  $10^{\circ}\text{N}$ , cyclonic vorticity intensifies (Fig. 4.8d) (perhaps as a result of a Rossby wave response (Gill, 1980) to the tropical Atlantic Marine ITCZ warming). These changes in lower-level vorticity to the north and to the south of the Caribbean basin lead to an intensification of the easterly rotational wind from the SNA into the Caribbean Sea. Also, to the southwest of the Caribbean (over Costa Rica and Panama) there is an increase of the cyclonic relative vorticity, further intensifying the rotational easterly wind from the central Caribbean to the eastern coast of Central America (Fig. 4.8d). Additionally, having an increase in

convergence to the west and an increase in divergence to the east, a stronger easterly irrotational wind over the western Caribbean is also part of the CBNLLJ intensification from May to June (Fig. 4.8c).

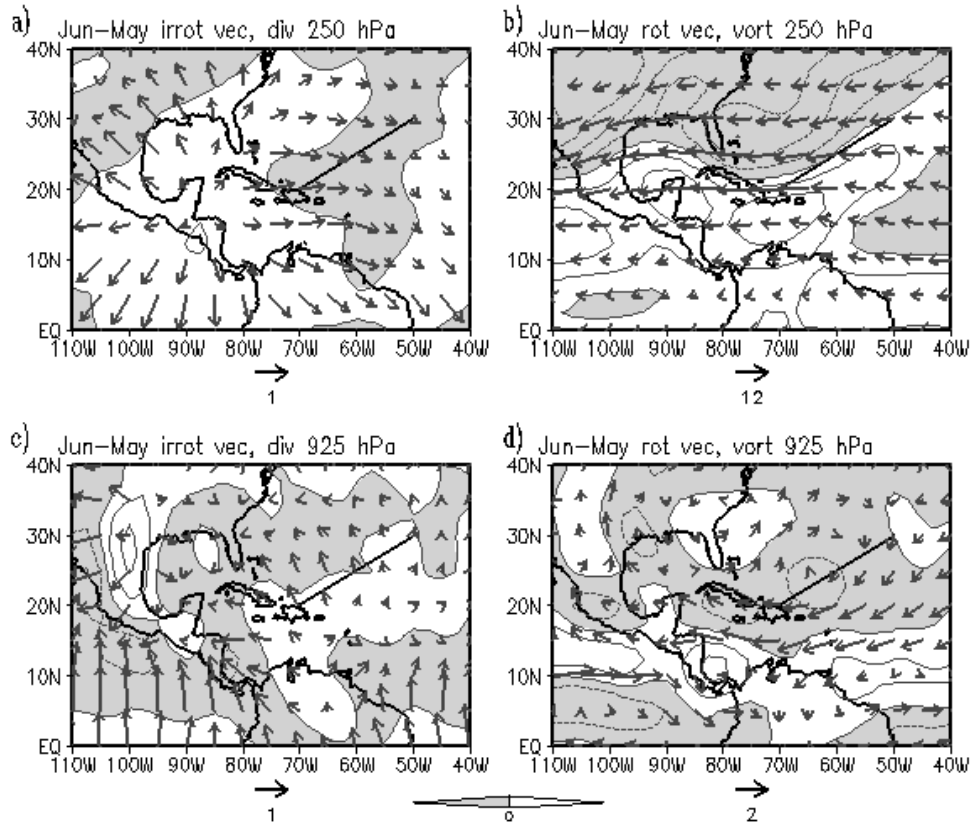


**Figure 4.8.** June-May difference of the irrotational wind and its divergence (left panels) and of the rotational wind and its vorticity (right panels) at 250 hPa (upper panels) and 925 hPa (lower panels) from the NCEP/NCAR Reanalysis. Reference arrow in m/s. Negative values are shaded. A reference line has been drawn from 20°N, 70°W to 30°N, 50°W. Contour interval for the difference in divergence is  $2 \text{ s}^{-1} \times 10^{-6}$ , for the difference in vorticity at 250 hPa is  $4 \text{ s}^{-1} \times 10^{-6}$  and at 925 hPa is  $3 \text{ s}^{-1} \times 10^{-6}$ .

#### 4.3.2 Summer Caribbean minimum of precipitation

During July the ITCZ is strongest over the tropical North Atlantic, Central America and the tropical northeastern Pacific (Fig. 4.9). However, as observed in Fig. 4.9, the precipitation over the Caribbean Sea is not as intense as the precipitation

over Central America. The spatial pattern of precipitation rate for July shows a relative spatial minimum of precipitation centered over the Caribbean Sea. The precipitation increases from the central Caribbean Sea to the west reaching values greater than 8 mm/day west of Central America corresponding to the ITCZ. The relative spatial minimum of precipitation over the Caribbean Sea coexists with sea surface temperatures (SSTs) greater than 27.5°C (Figs. 4.9a and 4.9c). SSTs greater than 27.5°C are considered over the threshold for convective precipitation in other tropical regions (Graham and Barnett, 1987). However, for the Caribbean Sea, even though the SSTs are greater than 27.5°C the precipitation is a relative minimum with less than 2 mm/day. Other adjacent regions to the Caribbean Sea with relatively weak precipitation and SSTs greater than 28.5°C are the Gulf of Mexico and the region north of the Greater Antilles and south of 27°N (Figs. 4.9a, 4.9c).

These regions of weak precipitation, in particular the Caribbean Sea and the Gulf of Mexico, are collocated with regions of subsidence. Figure 4.9b presents the vertical velocity at 850 hPa from the ERA-40. There is descending motion over the Caribbean Sea, the Gulf of Mexico and north of the Greater Antilles. Over the adjacent land areas, i.e., Mexico, Central America and South America, there is ascending motion; an exception is the western side of Central America at about 13°N where there is descending motion. The subsidence in the Gulf of Mexico is stronger at about 25°N below 700 hPa and in the Caribbean is stronger between 66°W and 74°W below 500 hPa.

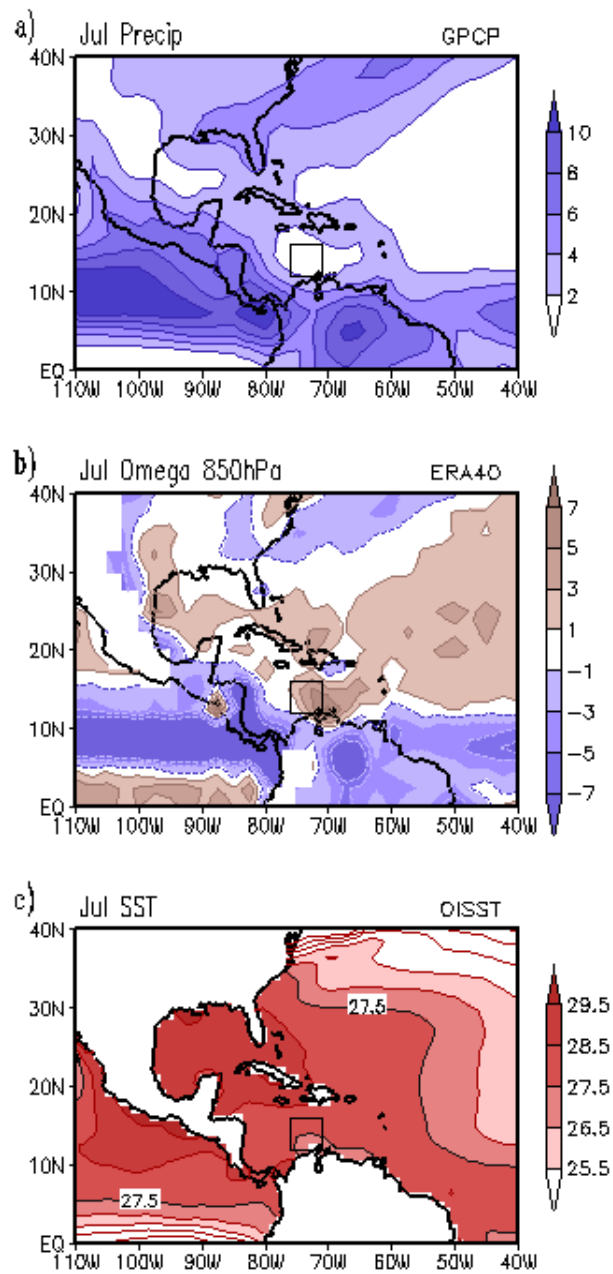


**Figure 4.9.** (a) July precipitation (mm/day), (b) vertical pressure velocity at 850 hPa (Pa/s x 100) and (c) sea surface temperature (°C). The rectangle delineates the area from 12°N to 16°N and from 71°W to 76°W.



The regions of subsidence are also regions of moisture flux divergence (MFD) vertically integrated below 700 hPa (from NARR). MFD extends throughout most of the Caribbean Sea, the Gulf of Mexico and north of the Greater Antilles (not presented). On the other hand, there is moisture flux convergence (MFC) over adjacent land areas. A region of strong MFD in the Caribbean Sea is between 70°W and 74°W. In fact, over the Caribbean, the zonal moisture divergence dominates in the domain of the CBNLLJ. Between 11°N and 18°N (i.e., between the southern and northern boundaries of the Caribbean Sea) the MFD below the 700-hPa level extends from the Lesser Antilles (at about 61°W) to 79°W. Out of this region of MFD, the zonal divergence dominates over the opposing meridional convergence from 66°W to 74°W, a region that also corresponds to the CBNLLJ. This indicates that the zonal divergence (and the easterlies spatial intensification) is the main contributor to the total MFD in the region of the CBNLLJ. The strengthening of the Caribbean easterlies as a LLJ is directly related to stronger MFD.

The Caribbean minimum of precipitation is not only a spatial feature, but also a temporal feature. Although the precipitation over the Caribbean is scarce year round (in comparison to the ITCZ), the Caribbean precipitation (from GPCP) between 70°W and 75°W decreases from May to July (Fig. 4.10a) as the CBNLLJ intensifies, and then increases from July to August (not presented) as the CBNLLJ weakens. Additionally, from May to July there is stronger diabatic cooling and stronger subsidence over the Caribbean Sea (Fig. 4.10b). Figure 4.10b shows the diabatic heating and wind change from May to July. The diabatic heating was calculated as the residual from the thermodynamic equation using ERA-40 data. The subsidence

over the Caribbean Sea is related to the MFD, to the suppression of precipitation and to the diabatic cooling by entraining cooler and dryer air from above into the lower levels of the Caribbean atmosphere.

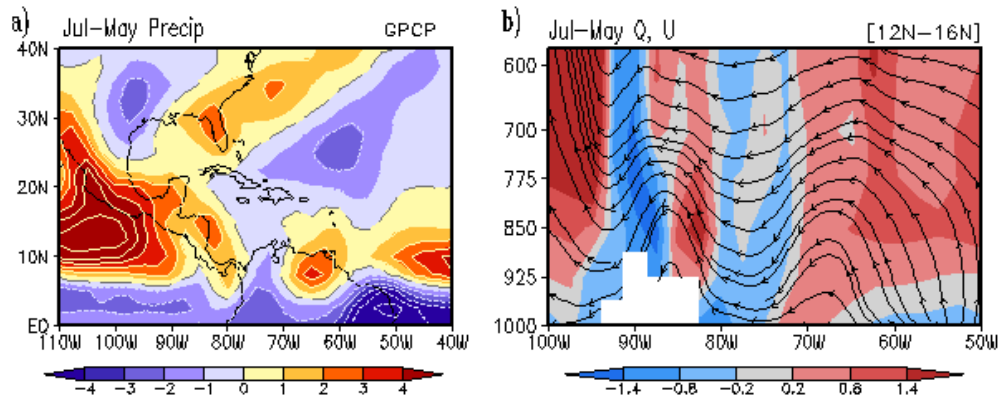


**Figure 4.10.** (a) July-May difference of precipitation (mm/day) from GPCP. Contour interval is 1 mm/day. (b) Pressure-longitude cross-section of the July-May difference of diabatic heating ( $\text{K/s} \times 10^5$ , shades) and the zonal and vertical wind (streamlines) averaged from  $12^\circ\text{N}$  to  $16^\circ\text{N}$  from ERA-40. In (b) the mountains of Central America are in white between  $85^\circ\text{W}$  and  $90^\circ\text{W}$ .

On the other hand, over the eastern slope of Central America there is a combination of ascending motion, diabatic heating and moisture flux convergence reflected as a strong precipitation rate. Between  $81^\circ\text{W}$  and  $85^\circ\text{W}$ , over the Caribbean side of the Central American cordillera, the precipitation has increased more than 2 mm/day from May to July (Fig. 4.10a). As the easterlies encounter the Central American landmass and deflect upward, enhancements of convergence and convection occur, leading to more precipitation and more diabatic heating (Fig. 4.10). The diabatic heating increases more than  $2 \times 10^{-5} \text{ K/s}$  between 775 hPa and 925 hPa (Fig. 4.10b) contrasting with the diabatic cooling over the central Caribbean. The intensification of the Caribbean east-west gradient of diabatic heating coincides with

a monsoon-like summer strengthening of the easterly wind. In fact, the 925-hPa zonal component of the divergent (irrotational) wind over the western Caribbean has become more easterly from May to June (as discussed above).

The strengthening (or onset) of the CBNLLJ from May to July is related to a direct circulation that influences the western Central America (northeastern tropical Pacific) mid-summer drought (MSD). The western Central America MSD occurs from June to July (Magaña et al. 1999) lagging the Caribbean MSD. Over 90°W, the western side of Central America shows a decrease in diabatic heating of  $\sim 1.4 \times 10^{-5}$  K/s and greater descending motion. Essentially, as the CBNLLJ intensifies from May to June and then to July, the easterlies reach the Central American mountains and also the monsoon heating. The easterlies deflect upward and subside over the western side of Central America (Fig. 4.10b). The subsidence most likely inhibits precipitation resulting in less diabatic heating. This confirms the findings of Magaña and Caetano (2005). To the west of the MSD region, the continuing intensification of the ITCZ is observed (at about 100°W) with positive heating change and greater upward motion.

Throughout the year the precipitation in the Caribbean region is anti-correlated with the easterly Caribbean low-level wind. Figure 4.11 presents the correlation between the seasonal cycle of Caribbean 925-hPa zonal wind (averaged from 12°N to 16°N and from 71°W to 76°W) and the seasonal cycle of precipitation. It is observed that with an intensification of the easterly wind there is a weakening of precipitation over the Caribbean Sea centralized in the region of maximum easterlies, the CBNLLJ. Two other areas of strong anti-correlation are the subtropical North Atlantic and the Gulf of Mexico. The precipitation in the SNA (centered at 20°N, 55°W) is anti-

correlated with the stronger easterly wind that extends from that region. In contrast, the precipitation in the southeastern United States is positively correlated with a stronger flow from the Caribbean that extends to the Gulf of Mexico providing moisture to the southeastern United States.

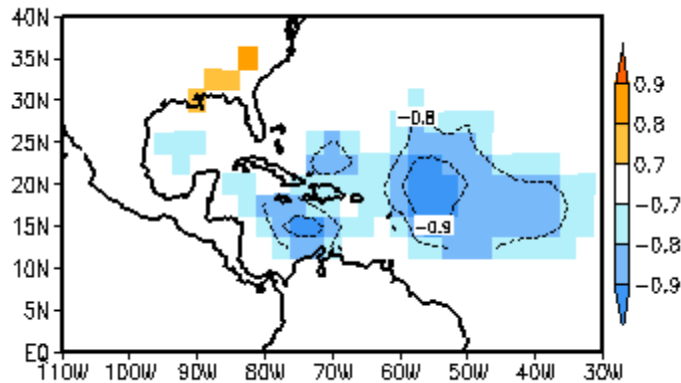


**Figure 4.11. Correlation between the 12-month seasonal cycle of precipitation and the 12-month seasonal cycle of Caribbean 925-hPa zonal wind index. The precipitation is from GPCP. The Caribbean 925-hPa zonal wind index (multiplied by -1) is the area-average between 12°N and 16°N and between 71°W and 76°W from NARR. Correlation coefficients significant at the 95% level are shown.**

## Chapter 5 : Interannual Variability and Changes

### 5.1 Summer interannual variability

The interannual variability of the CBNLLJ is analyzed for boreal summer months. The standard deviation of the monthly anomalies of the zonal component of the wind is computed as a measure of interannual variability. For the months of June through September the standard deviation is greater at 925 hPa and roughly in the area bounded by 12-17°N and 70-80°W (Fig. 5.1). The variability of the CBNLLJ is then summarized as an index of the anomalies of the 925-hPa zonal component of the wind averaged over the region 12-17°N and 70-80°W. The time series of the CBNLLJ anomaly indices is shown in Fig. 5.2. Spectral analysis (not presented) of the June-August anomalies has a peak at 3.5 years (significant at the 90% level). Other peaks lie in the lower-frequency domain, i.e., a peak at 11 years and another at 9 years.

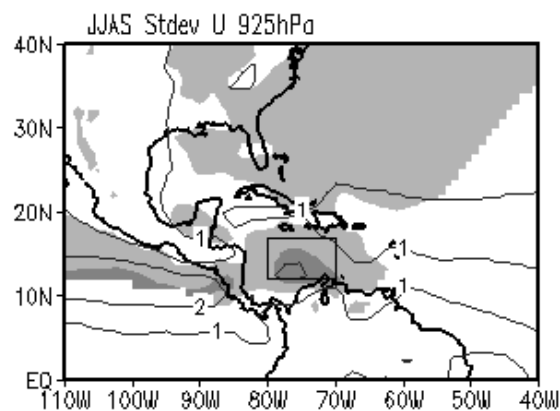


**Figure 5.1. June-to-September average standard deviation of the 925-hPa zonal wind anomalies (m/s) from NARR (shades) and ERA-40 (contours).**

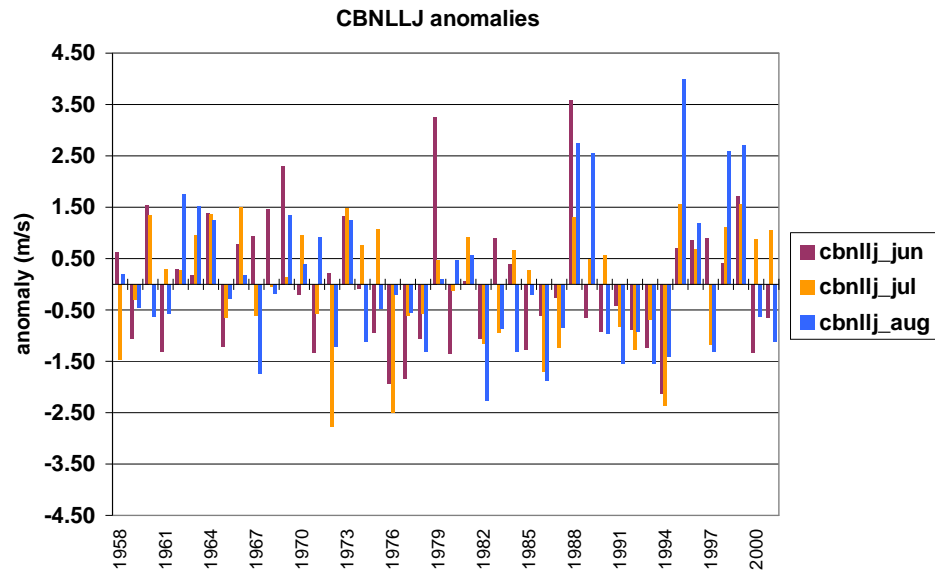


**Figure 5.2. Time series (bars) of Caribbean LLJ anomalies (m/s) for June, July and August from ERA-40.**

Regression analyses are performed to analyze the structure of interannual variability of the CBNLLJ during summer. Initially, the results for the July CBNLLJ analysis will be presented. The month of July is chosen because it is in July when the CBNLLJ is at its peak. Then, the changes with decades of the CBNLLJ will be presented and discussed for the summer months separately. The regression coefficients were multiplied by the non-dimensional CBNLLJ standard deviation (as a scaling factor) of the respective month. The regressions are shown with respect to a decrease in easterly wind; hence the discussion is based on a weaker-than-average CBNLLJ.

As observed from Fig. 5.3a, in July a weakening of the CBNLLJ is observed as part of a weakening of the flow from the tropical Atlantic (east of the Caribbean Sea) crossing the Caribbean and Central America and extending to the northeastern

tropical Pacific. There is a weakening of the flow into the Gulf of Mexico and into the gulf states of USA that connects to the Great Plains (compare with the July climatology shown in Fig. 4.1b). The changes in the wind in the Caribbean region correspond to a decrease in the meridional SLP gradient across the Caribbean region and a warming of the Caribbean SSTs (Fig 5.4 middle).

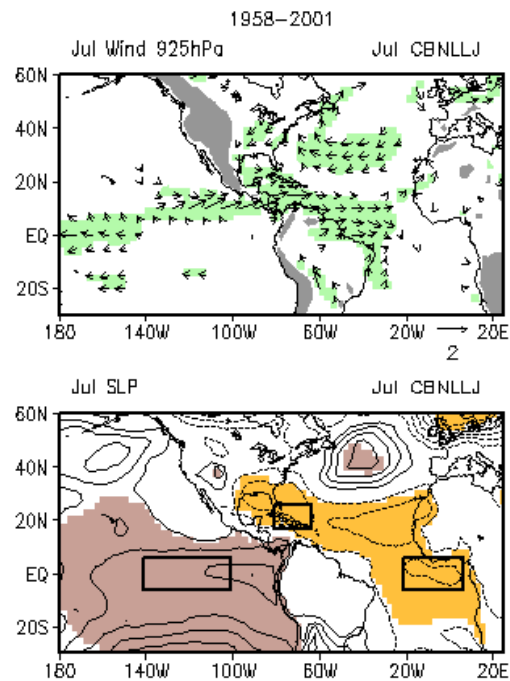


**Figure 5.3. July 925-hPa wind anomaly vector (m/s, top) and SLPA (hPa, bottom) regressed onto the Caribbean LLJ July anomaly index (i.e., 925-hPa zonal wind anomalies averaged over 12-17°N and 70-80°W). Contour interval of SLPA is 0.2 hPa. Negative SLPA are dashed contours and positive SLPA are solid contours. Values statistically significant at the 95% level are shaded. The regions in the equatorial Pacific, Caribbean and equatorial Atlantic indicated by a rectangle in the bottom figure were used for area-averages of SLPA.**

Figure 5.3 shows the linear regression coefficients resulting from July SLP anomalies regressed on the July CBNLLJ anomaly index. Over the Intra-Americas Sea (IAS; Caribbean Sea and Gulf of Mexico regions) the surface pressure has weakened (compare with the July climatology shown in Fig 4.4b). The SLP

anomalous pattern shows a meridional gradient from north to south across the northeastern tropical Pacific, Central America and the Caribbean Sea. This weakening of the meridional SLP gradient in July is part of a greater anomalous pattern with a decrease in pressure across the tropical Atlantic between 30°N and 15°S and an increase in pressure over the tropical Pacific.

Over the tropical Atlantic the changes in pressure are greater in the subtropical North Atlantic between 10°N and 30°N. Another Atlantic region of significant SLP anomalies is the central-eastern equatorial Atlantic region. Over the Pacific the changes in pressure are positive from the western South American coast to the west and greater over the equatorial region. Hence, because of the slanted northwest to southeast orientation of the Central America isthmus, with positive pressure anomalies south of Central America and negative pressure anomalies over the IAS, the meridional pressure gradient across Central America and the Caribbean regions is weakened as well as the CBNLLJ.

Similarly, there is an inter-basin SST anomaly (SSTA) pattern associated with changes in the intensity of the CBNLLJ during summer. The SSTAs regressed onto the CBNLLJ anomaly index for July, displayed in Fig. 5.4, shows negative (cooler) SSTAs in the tropical Pacific and positive (warmer) SSTAs in the tropical Atlantic. The negative SSTAs in the Pacific are strongest in the equatorial Pacific Niño3 and Niño3.4 regions and lead the July CBNLLJ by 2 months (Fig 5.4). The positive anomalies in the tropical Atlantic are strong in the equatorial region and in the tropical North Atlantic, in particular the Caribbean Sea region. However, one and



two months before July CBNLLJ anomalies, the Caribbean Sea does not show significant SSTAs.

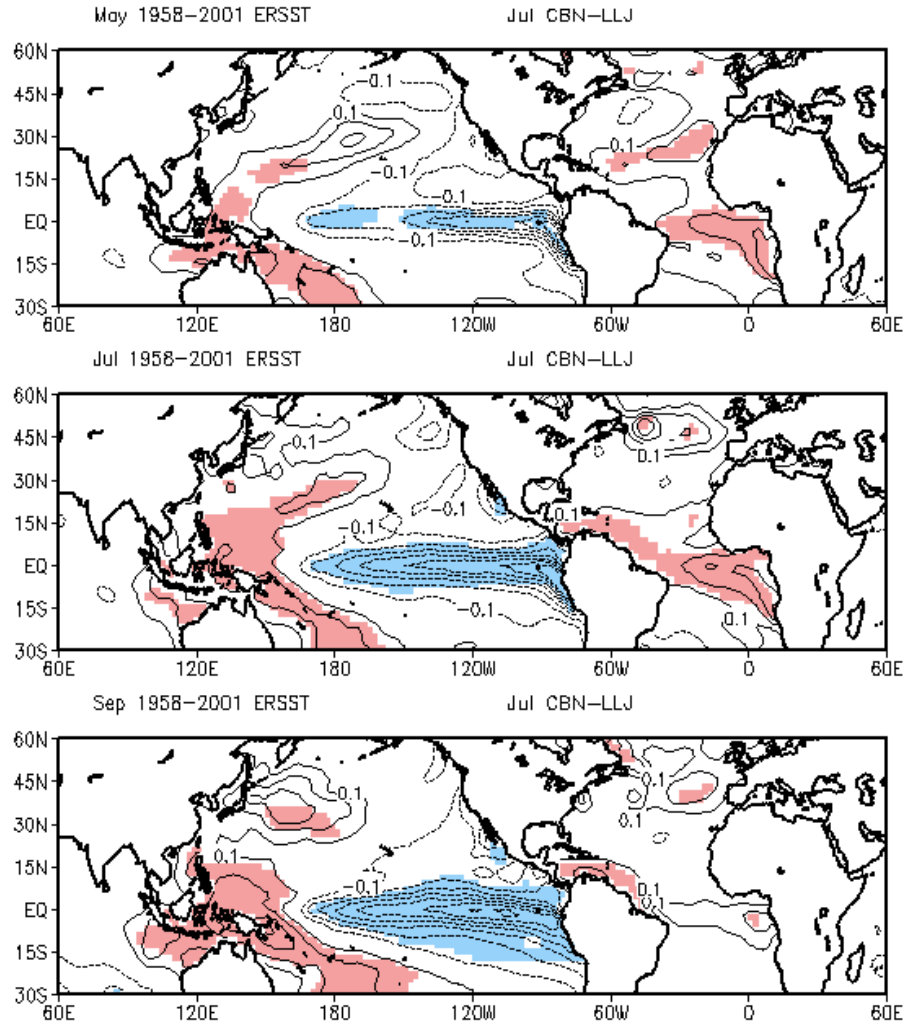


**Figure 5.4.** May (top), July (middle) and September (bottom) SSTA ( $^{\circ}\text{C}$ ) regressed onto July CBNLLJ anomaly index. Contour interval is  $0.1^{\circ}\text{C}$

The lack of significant Caribbean SSTAs before the July CBNLLJ anomalies (Fig. 5.4) is indication that the IAS warm pool is not influencing the July CBNLLJ with lead time. Also, the SLPAs leading the July CBNLLJ anomalies (not presented)

show strong positive anomalies over the tropical Pacific, but no significant anomalies over the IAS. Rather, the IAS warm pool responds to the summer CBNLLJ as observed from the SSTAs two months after the July CBNLLJ anomalies (Fig. 5.4).

The divergent and rotational components of the wind at 925 hPa and 250 hPa further confirm the regions of remote forcing (Fig. 5.5). The anomalous irrotational (divergent) component of the flow and the velocity potential anomalies at the lower level (925 hPa) diverge from the tropical Pacific and converge towards the tropical North Atlantic (TNA) and the IAS as is expected from the cold SSTAs in the Pacific and the warm SSTAs in the Atlantic. The weakening of the CBNLLJ, then, has contributions from the anomalies of the divergent flow. At the upper level (250 hPa) the divergent flow converges towards the tropical Pacific and diverges from the TNA indicating that there is a convergence cell from the Atlantic to the Pacific with the CBNLLJ as a corridor that unifies the two basins at the lower levels.

Nonetheless, the greatest contribution to the CBNLLJ comes from the rotational component of the wind (Fig 5.5). At the lower and upper levels the rotational wind anomalies are mostly zonal in the Caribbean. With westerly anomalies at the lower level (a weaker CBNLLJ) and easterly anomalies at the upper (250-hPa) level, a weaker vertical shear of the zonal wind develops in the Caribbean region of which the CBNLLJ is part of. Through its contribution to changes in the wind vertical shear, the CBNLLJ may modulate the Caribbean precipitation.

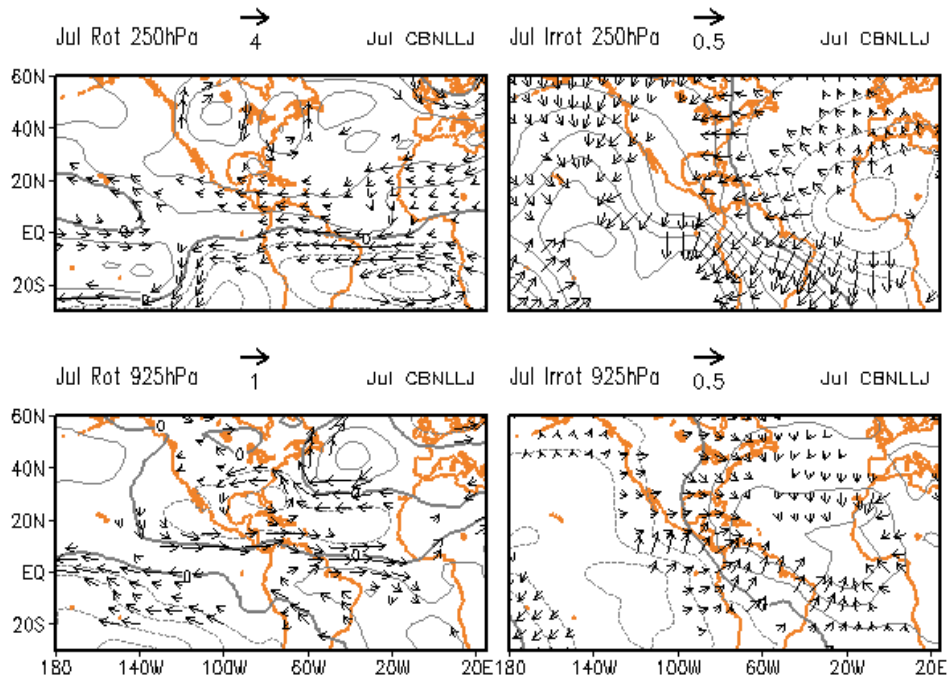


**Figure 5.5.** July (left) rotational and (right) irrotational component of the wind (m/s) and (left) streamfunction (1/s) and (right) velocity potential (1/s) anomalies regressed onto July Caribbean LLJ anomaly index. Top panels are for 250-hPa level and bottom panels are for 925-hPa level. A reference arrow is displayed at the top of each panel. Negative anomalies are dashed contours and positive anomalies are solid contours. Contour interval of 250-hPa streamfunction is  $1e+6$ ; of 925-hPa streamfunction is  $4e+5$ ; of 250-hPa velocity potential is  $2e+5$ ; of 925-hPa velocity potential is  $2e+5$ .

In fact, the July precipitation anomalies regressed onto the July CBNLLJ index show that precipitation increases in the central Caribbean for a weaker CBNLLJ (Fig. 5.6). This increase is in part due to the weaker wind vertical shear between the upper levels (250 hPa) and the lower levels (925 hPa) as shown in Fig. 5.5. Additionally, with a weaker CBNLLJ there is weaker moisture flux divergence in the Caribbean and tropical North Atlantic regions. The weaker moisture flux divergence allows an increase in the precipitation rate. Downwind of the jet, on the western part of the Caribbean, the magnitude of the moisture fluxes becomes weaker between 800 and 950 hPa (please refer to Fig. 4.6). Nonetheless, the zero-line of the meridional

moisture flux (the bifurcation) does not change in the vertical (except for very close to the surface below 950 hPa). Further downwind, over the Gulf of Mexico, the humidity increases but, given the weaker southerlies, the southerly moisture flux into the Gulf States is weaker. Even though there is greater precipitation in the mid-summer drought (MSD) region of Central America, the MSD (as the decrease in precipitation from June to July-August) is still present. The greater changes in the MSD under a weaker CBNLLJ occur in July.

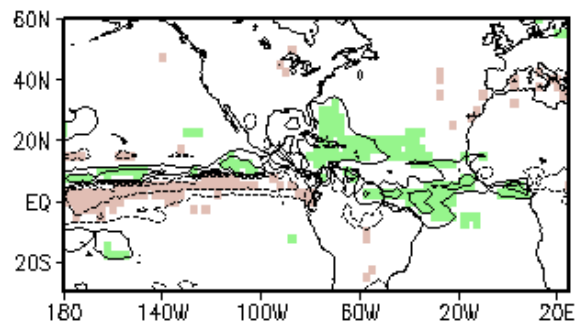


**Figure 5.6. July precipitation anomaly (mm) regressed onto the CBNLLJ July anomaly index. Contours are -0.3, -0.1, 0.1 and 0.3. Positive (negative) precipitation anomalies are solid (dashed) contours. Values statistically significant at the 95% level are shaded. Precipitation data is from ERA-40.**

In the Pacific the changes are those of a cold ENSO event with an increase in SLP and a decrease in SST. By quantifying the correlation between July CBNLLJ anomaly index and Niño3.4 anomaly index in the preceding and following months (Fig. 5.7), significant correlation is obtained with the Niño3.4 leading by three months (i.e. since April). The correlation between the leading Niño3.4 and July CBNLLJ peaks in June. There are also significant correlations for the July CBNLLJ anomalies and the following Niño3.4 conditions. However, these may be an artifact of the high persistence of Niño3.4 anomalies.

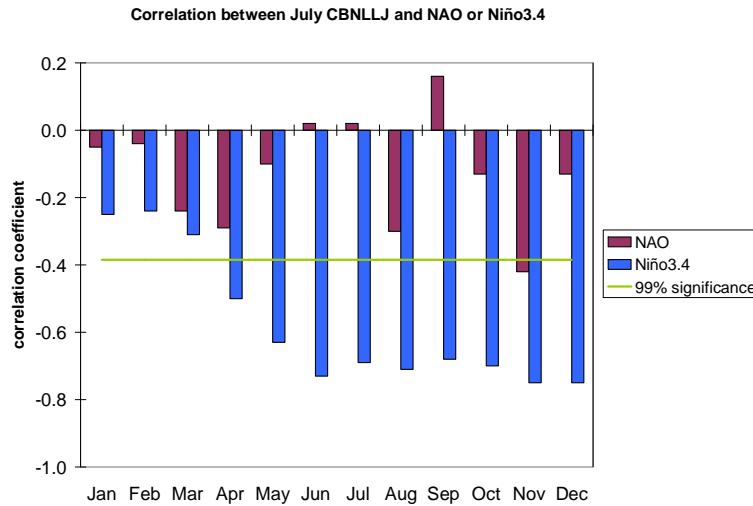


**Figure 5.7. Correlation between July CBNLLJ anomalies and the North Atlantic Oscillation index (NAO; violet bars) or the Niño3.4 index (blue bars) during previous, concurrent and posterior months.**

The correlation between the July CBNLLJ anomalies and the North Atlantic Oscillation index (Fig. 5.7) is very weak for concurrent NAO, leading NAO and lagging NAO. However, the correlation between the Atlantic Multidecadal Oscillation (AMO) and the summer CBNLLJ is higher.

To correlate the summer AMO and the summer CBNLLJ, a 5-year running mean was applied to the June-July-August CBNLLJ anomalies. The correlation coefficient for the entire 1958-2001 period is 0.5, which is higher than the correlation between the NAO and the CBNLLJ. The influence of the AMO, as discussed in the introduction chapter, would be through the influence on the pressure of the tropical North Atlantic. As the AMO is in a warming phase, the pressure north of the Greater Antilles weakens (Knight et al, 2006). The decrease in pressure weakens the northward gradient of pressure across the Caribbean resulting in a weaker CBNLLJ.

Overall, the observations described above pinpoint to the July negative SLPAs in the IAS region being a response to the remote forcing from the tropical Pacific and the tropical North Atlantic augmented by a positive feedback in the Caribbean region. The changes in the IAS region are related to the Pacific by modifying the Walker and Hadley atmospheric circulations that link the IAS with the tropical Pacific. As weaker uprising motion occurs in the tropical Pacific, the cell that connects to the Atlantic is weakened and stronger uprising motion occurs in the IAS (in particular weaker low-level sinking over the Gulf of Mexico region). As a result, surface pressure north of the Caribbean region decreases and the low-level easterlies are weakened. As the low-level easterlies weaken in July, weaker upwelling (not presented) and weaker thermodynamic cooling increase the SSTs in the Caribbean. The positive Caribbean SSTAs further contribute to decrease the SLP anomalies. Over the Pacific, the SSTAs are colder and the SLP stays higher than climatology. The weaker meridional pressure gradient across Central America and the Caribbean further weakens the CBNLLJ.

The CBNLLJ studies mentioned in the introduction (Wang, 2007; Whyte et al, 2007; Muñoz et al, 2007) are based on different periods and different months of the summer. Wang (2007) focuses on the CBNLLJ anomalies of August and September for the period from 1950 to 2006. Whyte et al (2007) focus on the CBNLLJ anomalies of June and July for the period from 1958 to 1998. Muñoz et al (2007) focus on the CBNLLJ anomalies of July-August for the period from 1979 to 2001 as this is the common period between the North American Regional Reanalysis (NARR) and the ECMWF 40-year Reanalysis (ERA-40).

Additionally, previous research has not addressed whether or not the summer CBNLLJ variability has changed with epoch. First I ask, has the CBNLLJ variability changed? Have the changes been mostly during the onset, peak or decay month of the CBNLLJ? Furthermore, how are the changes related to changes in the remote forcing? Since, the CBNLLJ has been studied previously for the summer months of June through September, I analyze the variability of the Caribbean 925-hPa zonal wind for those summer months.

### 5.2 Changes in the Caribbean LLJ strength and persistence

The autocorrelation of the CBNLLJ anomaly index in July with those of previous and subsequent months is calculated to determine the persistence of CBNLLJ anomalies. Figure 5.8 presents the correlation between the CBNLLJ anomaly index in July and that for May through October separately, from the ERA-40 Reanalyses. For 21 years, the 95% (99%) level of significance is a correlation coefficient of 0.43 (0.55). For the earlier period 1958-1978 the autocorrelation of July CBNLLJ anomalies is not significant throughout the boreal summer. Only the correlation between July and September CBNLLJ anomalies is significant for the period 1958-1978.

However, for the latter period 1981-2001, the autocorrelation of July CBNLLJ anomalies is significant at the 95% (99%) level from June throughout September (from July throughout September). Similar results were obtained from the NARR CBNLLJ index. Indeed, a 21-year running correlation of CBNLLJ anomalies between summer months (not presented) shows that the July and August correlation became significant after the period centered on 1978 and reached much higher values

after the period centered on 1984. The period centered on 1984 is also notable for the correlation between June and July; and between August and September increases and becomes statistically significant.

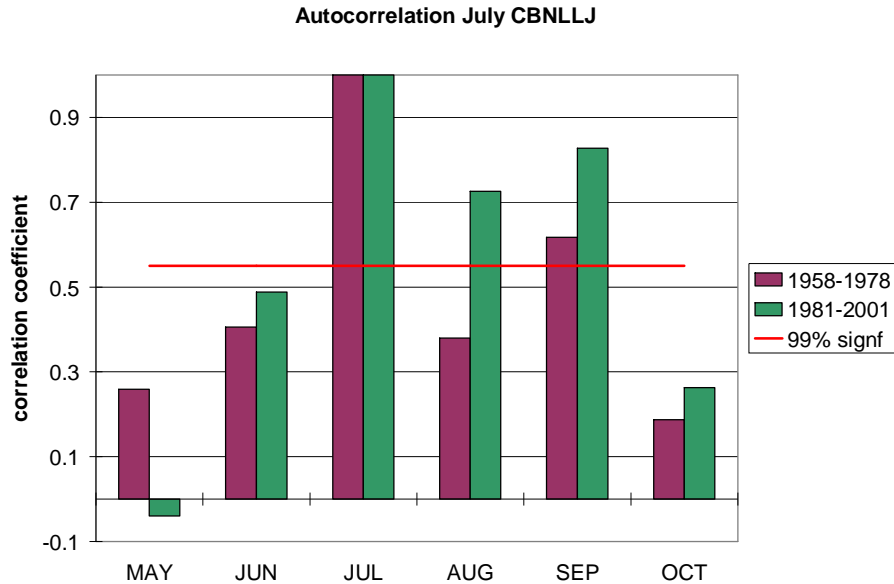


**Figure 5.8. Autocorrelation of July Caribbean LLJ anomalies with summer months for two different periods: 1958-1978, 1981-2001. A line showing the 99% significance level is shown.**

These indicate that for the latter decades (i.e., 1981-2001) the July CBNLLJ monthly anomalies have had greater persistence throughout the boreal summer. This persistence is important given the potential effect of stronger (weaker) zonal windstress over the Caribbean Sea and, in turn, stronger (weaker) upwelling and cooler (warmer) SSTs (among other influences).

A question then is, have the CBNLLJ events changed in magnitude with the consequence of a greater influence on the regional climate anomalies? To answer this question, the computation of the 21-year running standard deviation of June, July, August and September CBNLLJ anomalies is analyzed.



The standard deviation of the CBNLLJ anomalies in June and July has not changed as much as it has in August and September. The 21-year running standard deviation for the summer months is shown in Fig. 5.9. It can be observed that the standard deviation for July is rather constant at about 1.15 m/s. Similarly, the June standard deviation does not vary much throughout the period 1958-2001 being most of time between 1.4 and 1.5 m/s. On the other hand, the standard deviation of August and September changes significantly and has an increasing trend from 1958 to 2001.

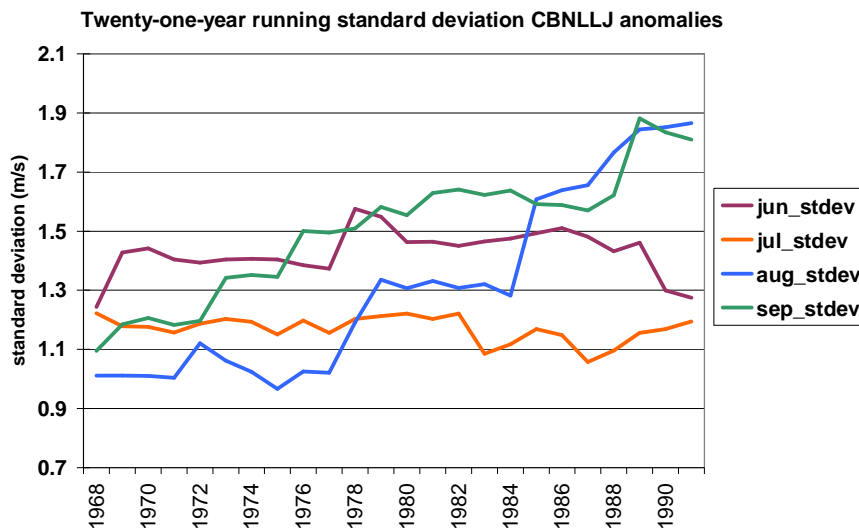


**Figure 5.9. Twenty-one-year running standard deviation (m/s) of CBNLLJ anomalies for June, July, August and September.**

For August, the standard deviation was about 1 m/s and lower than the July standard deviation before the period centered on 1978. After the period centered on 1978 the standard deviation of August CBNLLJ anomalies increases and surpasses the standard deviation of the July CBNLLJ (Fig. 5.9). The August standard deviation continued increasing and reached values of 1.85 m/s for the period centered on 1990. Hence, the August standard deviation almost doubled from the early 1960's to the late

1990's. Using an 11-year window, the August standard deviation increases more abruptly in the period centered on the late 1970's and the mid-1980's. The September standard deviation also increased but from 1.2 to 1.8 m/s. Hence, the August variability has increased in terms of the magnitude of the events.

The increasing standard deviation indicates that the late summer CBNLLJ events have become stronger from 1958 to 2001. This is observed from the histogram of Caribbean 925-hPa zonal wind anomalies for June-July (early summer) and August-September (late summer) (Fig. 5.10). The distributions of anomalies for the August-September plots show an increase in extreme events in the 1979-2001 period.

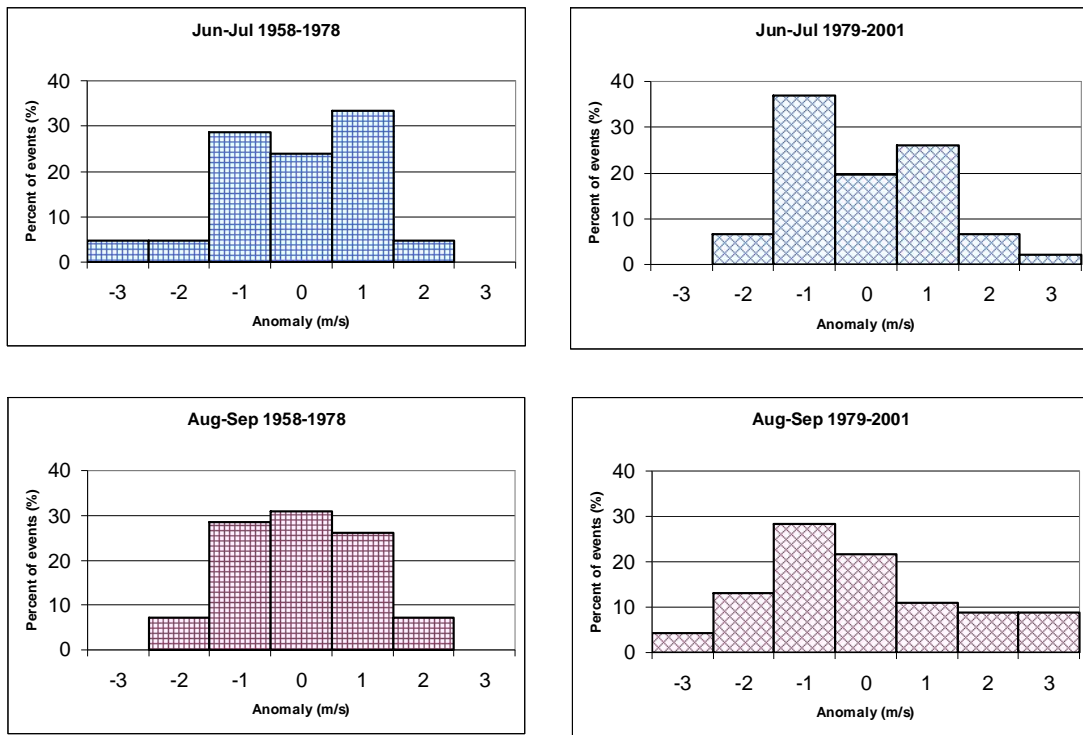


**Figure 5.10. Histograms of June-July (top) and August-September (bottom) CBNLLJ anomalies between the periods 1958-1978 (left) and 1979-2001 (right). The x-axis indicates the value of the center of the bin (e.g., 0 for the bin from -0.5 to 0.5). The y-axis indicates the percentage of events for each bin.**

As a check of the increasing standard deviation of the CBNLLJ I performed an Empirical Orthogonal Analysis (EOF) on June, July and August monthly anomalies. The main mode (EOF-1) of Caribbean 925-hPa zonal wind is the modulation of the CBNLLJ. EOF-1 has 73% of explained variance. The 21-year running standard deviation for June, July and August of PC-1 are similar to the standard deviation of the CBNLLJ indices. That is to say, June and July show a steady standard deviation whereas August shows an increasing standard deviation. The spectrum of PC-1 has a peak at 3.5 years. Another peak at 11 years does not reach the significance level. A different EOF with a modulation of the CBNLLJ was EOF-5 with a very modest 2% explained variance and spectral peaks at 7.0 years and 3.6 years.

Something to consider is the integration of satellite observations after 1978 in the reanalysis (Uppala et al, 2005). This may have introduced a bias in the climate fields (including the Caribbean winds). Considering this, I also calculated the 21-year running standard deviation (not presented) of Caribbean zonal surface wind from COADS data. As stated in the methods chapter, COADS is based on consistent surface observations and is an empirical data set. The COADS Caribbean zonal wind also has an increasing standard deviation in August-September whereas the standard deviation for June-July does not increase with epoch which confirms the findings from the reanalysis CBNLLJ indices.

In general, the changes in ERA-40 CBNLLJ have been mainly in the August variability. For example, the correlation between August and September has increased from 0.1 centered on late 1960's to 0.7 centered on late 1980's. These increases in late-summer autocorrelation and standard deviation indicate that the

extreme CBNLLJ events have become longer and more extreme in large part because of the changes in the August CBNLLJ.

### 5.3 Changes in the remote forcing of the Caribbean LLJ

As it has been discussed above, the CBNLLJ is remotely forced by SLPA and SSTA inter-basin gradients. A question then is, what changes in the forcing have occurred that enforce longer extreme events in the CBNLLJ? To answer this question, an analysis of the SLPA and SSTA inter-basin relation is done from Pacific and Atlantic indices of SLPA and SSTA. The indices are area-averages of the equatorial Pacific, north Atlantic and equatorial Atlantic SLPAs and SSTAs and are defined in Tables 5.1 and 5.2 and (for the case of SLPA indices) are shown in Fig 5.3.

Table 5.1. Sea level pressure anomaly (SLPA) indices

<i>Region</i>	<i>Short name</i>	<i>Longitudes</i>	<i>Latitudes</i>
Equatorial Pacific	PAC	140°W - 100°W	5°S - 5°N
Caribbean	CBN	80°W - 65°W	17.5°N - 25°N
Equatorial Atlantic	EQATL	20°W - 5°E	5°S - 5°N

Table 5.2. Sea surface temperature anomaly (SSTA) indices

<i>Region</i>	<i>Short name</i>	<i>Longitudes</i>	<i>Latitudes</i>
Niño3.4	PAC	170°W - 120°W	5°S - 5°N
Tropical North Atlantic	TNA	62.5°W - 32.5°W	2.5°N - 22.5°N
Equatorial Atlantic	EQATL	17.5°W - 2.5°W	2.5°S - 2.5°N

A set of indices is correspondent to the inter-basin relation between the equatorial Pacific and the tropical North Atlantic (or Caribbean). Another set of indices is correspondent to the inter-basin relation between the equatorial Pacific and the

equatorial Atlantic. These inter-basin relations are analyzed with respect to the 21-year running correlation between the Pacific indices and the Atlantic indices.

For the SLPA indices, as observed from Fig. 5.11, the equatorial Pacific (PAC) SLPAs were positively correlated with the Caribbean (CBN) SLPAs for June throughout the entire 1958-2001 period. In contrast, the June PAC SLPAs were anti-correlated (although not statistically significant) with the July CBN SLPAs for most of the period. For July, however, the PAC SLPAs were not correlated with the CBN SLPAs for the earlier part of the period. It was after the period centered on 1978 when they reached a modest positive correlation. A negative trend is observed in the correlation between July PAC SLPAs and August CBN SLPAs that changes from being positively correlated before 1973 to being negatively correlated after 1973.

Furthermore, the correlation of PAC and CBN SLPA for August and September has a decreasing trend after the period centered on 1968 until the period centered on 1990. The negative trend in the correlation is stronger for the PAC and EQATL SLPAs (not presented) for all the summer months, i.e., June through September. It is after the late 1970's when the anti-correlation and hence the propitious forcing of the CBNLLJ establishes.

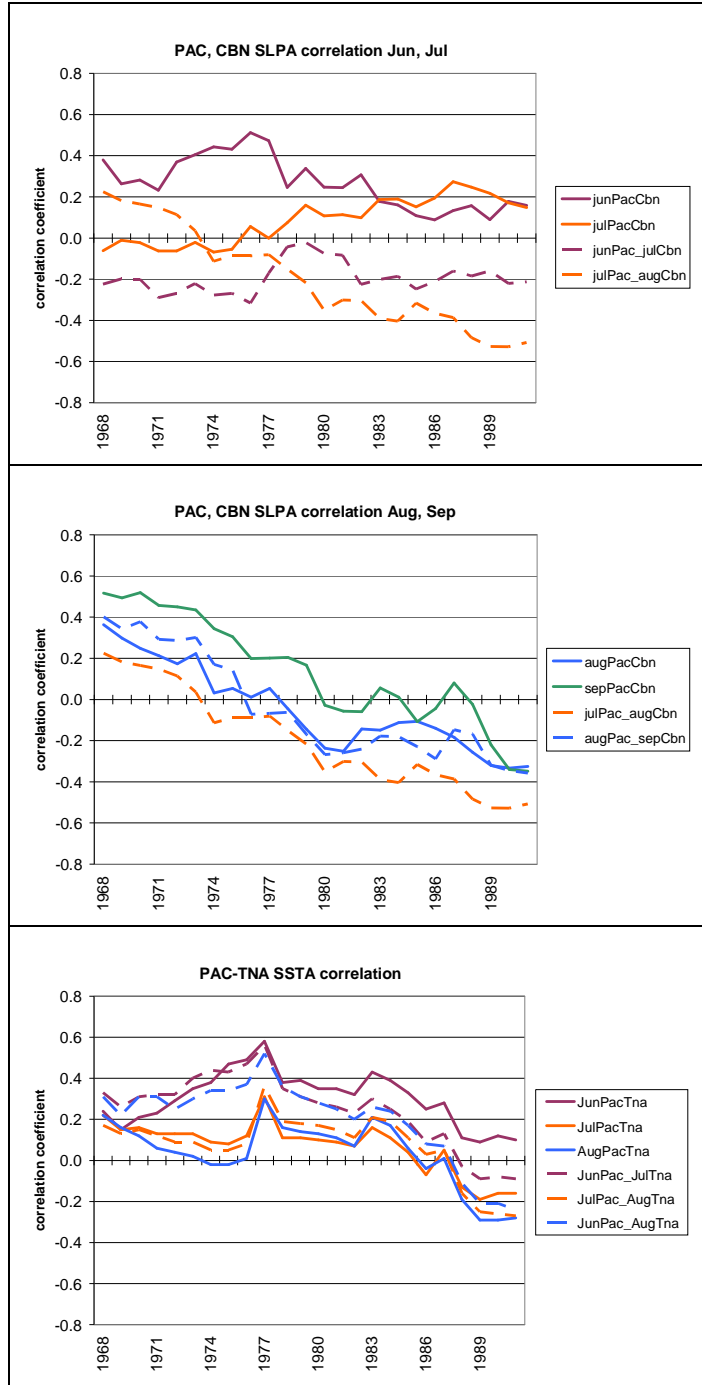


**Figure 5.11. Twenty-one-year correlation between SLP standardized anomalies of the equatorial Pacific and the Caribbean for (top) June, July; and (middle) August, September. (bottom) Twenty-one-year correlation between SST standardized anomalies of the equatorial Pacific and the tropical North Atlantic for June, July, August and September. Solid lines are concurrent correlations. Dashed lines are correlations with the Pacific index leading the Atlantic index.**

The SSTA parameters that have been associated with the intensity of the CBNLLJ anomalies are the SSTA gradients between: 1) the equatorial Pacific and the tropical North Atlantic (PAC-TNA) and 2) the equatorial Pacific and the equatorial Atlantic (PAC-EQATL). Similar to its atmospheric counterpart, the correlation between the PAC and TNA SSTA also change from being positively correlated to being negatively correlated in late-20<sup>th</sup> century (Fig. 5.11). Additionally, it has been after the late 1970's that the equatorial Pacific SSTA achieved a significant anti-correlation with the equatorial Atlantic SSTA (not presented). Also, the July and August SSTA gradient indices had greater standard deviation in the latter period. Hence the PAC-TNA SSTA difference has become more propitious for more extreme and longer-lasting CBNLLJ events.

These changes are corroborated by regression maps with the CBNLLJ index for two separate periods: 1958-1978, 1979-2001. Fig. 5.12 shows the regression of SLPA to the CBNLLJ anomaly index for June, July and August. For July, the inter-basin gradient is observed for both periods. Although, for the earlier period (1958-1978) the pressure anomalies over the North Atlantic centered at about 45°N, 30°W are significant whereas they are not significant for the latter period. For June and August, however, there is a clear difference in the Pacific anomalies between the two periods. For the earlier period, 1958-1978, June and August CBNLLJ anomalies are forced mostly by SLPA over the TNA in particular north of the Greater Antilles. However, for the latter period, the June and August CBNLLJ anomalies are influenced by PAC-ATL inter-basin gradients of SLPA.

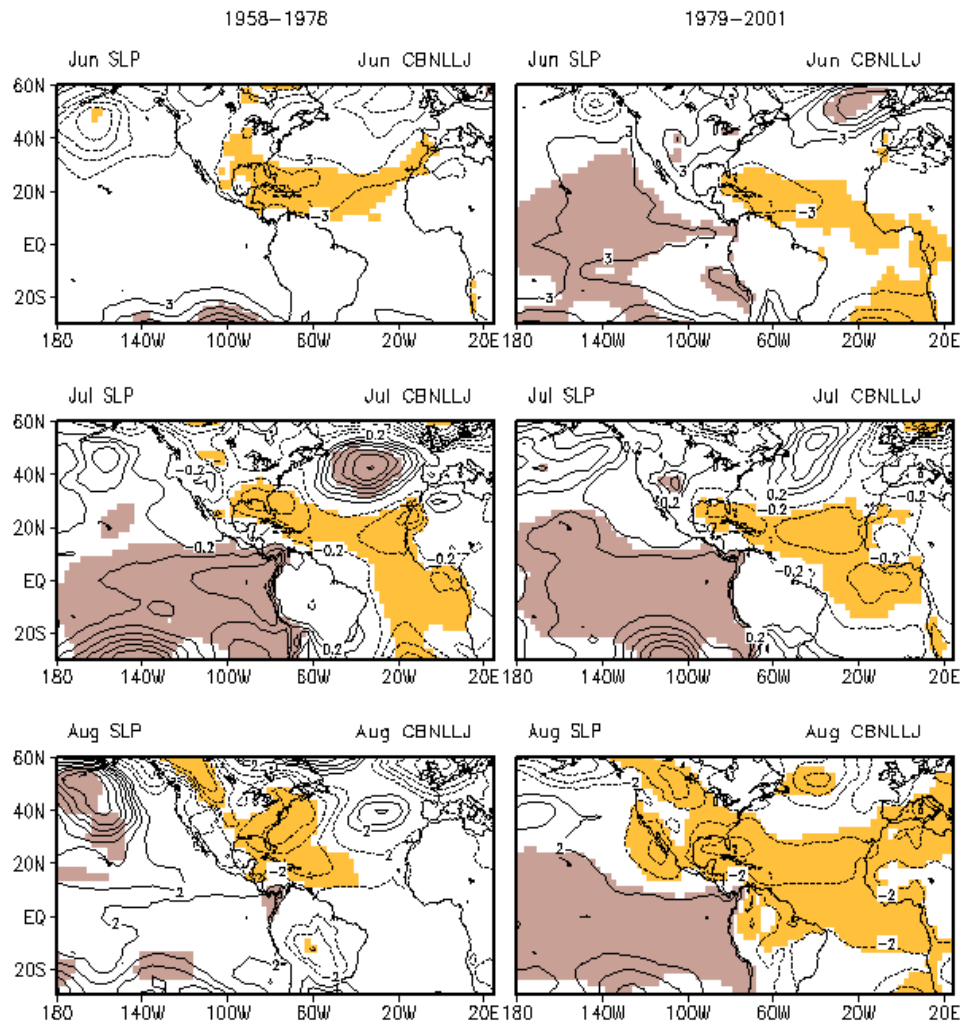


**Figure 5.12. SLPA (hPa) regressed to CBNLLJ anomaly index for (top) June, (middle) July and (bottom) August for the periods (left) 1958-1978 and (right) 1979-2001. Negative anomalies are dashed contours and positive anomalies are solid contours. Contour interval is 3 hPa for June, 0.2 hPa for July and 2 hPa for August. Shaded areas indicate values significant at the 95% level.**

The SSTAs related to the CBNLLJ anomalies for June, July and August are also different between the two periods (Fig. 5.13). For the earlier period (1958-1978) the June TNA forcing had significant anomalies mainly from the IAS, and the subtropical Pacific SSTAs had the same sign of the Atlantic SSTAs (i.e., there is no inter-basin SSTA gradient). July, during the earlier period, had a predominance of equatorial



Pacific SSTA, a minor SSTA inter-basin gradient and a lack of significant anomalies in the Caribbean basin. But for August in the earlier period, the SSTAs in the Intra-Americas Sea warm pool region are significant.

For June 1979-2001 (the latter period) the TNA SSTAs are the main forcing with some minor role of the equatorial Pacific. For July and August 1979-2001 the CBNLLJ is mostly influenced by the inter-basin SSTA gradient. In July and August, in the Caribbean Sea, the positive SSTAs are greater closer to the northern coast of South America. These Caribbean SSTAs are in consonance with weaker upwelling throughout the northern coast of South America and weaker thermodynamic cooling as the wind weakens and less evaporation occurs.

The CBNLLJ show less predictability before 1979 than after 1979 based on 2-month leading SSTAs (not presented). For June 1958-1978 the Caribbean SSTAs are significant 2 months in advance (i.e., in April). Whereas, for June 1979-2001 a SSTA tripole in the North Atlantic is significant 2 months in advance. For July 1958-1978 the May forcing is mainly from the eastern equatorial Pacific (Niño3 and Niño1+2) whereas for July 1979-2001 the leading SSTA in the Pacific are mainly in the western-central equatorial Pacific (Niño3.4 and Niño4), in the North Atlantic and in the equatorial Atlantic. For August 1958-1978 there is a lack of significant anomalies two months in advance whereas for August 1979-2001 there are significant anomalies in the equatorial Pacific and Atlantic and the North Atlantic.

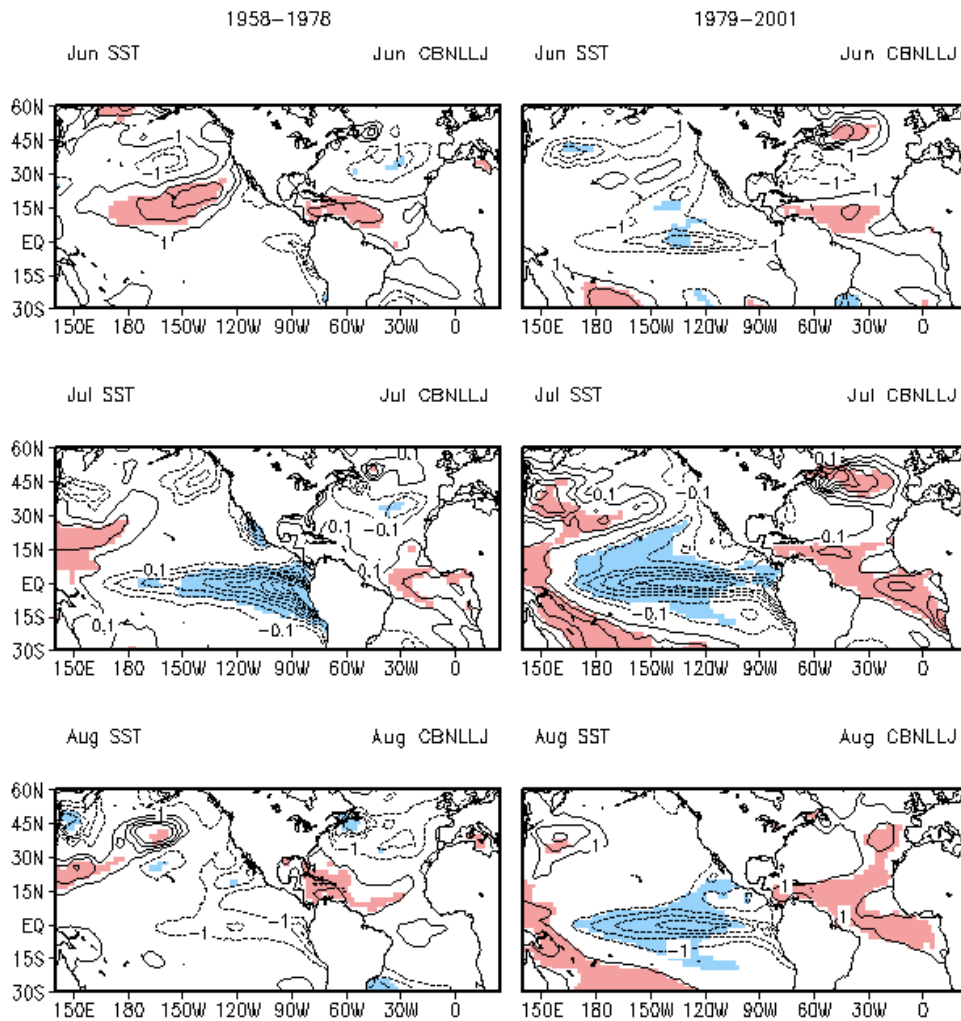


**Figure 5.13. Same as previous figure but for SSTA (°C). Contour interval is 1°C for June, 0.1°C for July and 1°C for August.**

The trend to a negative correlation between the Pacific and Atlantic basins (an inter-basin SSTA gradient) is a reflection of changes in each basin. Fig. 5.14 shows the regions of significant difference between the correlations of the earlier and latter periods. It is observed that there is significant difference in the tropics and subtropics of the Pacific and in the North Atlantic.

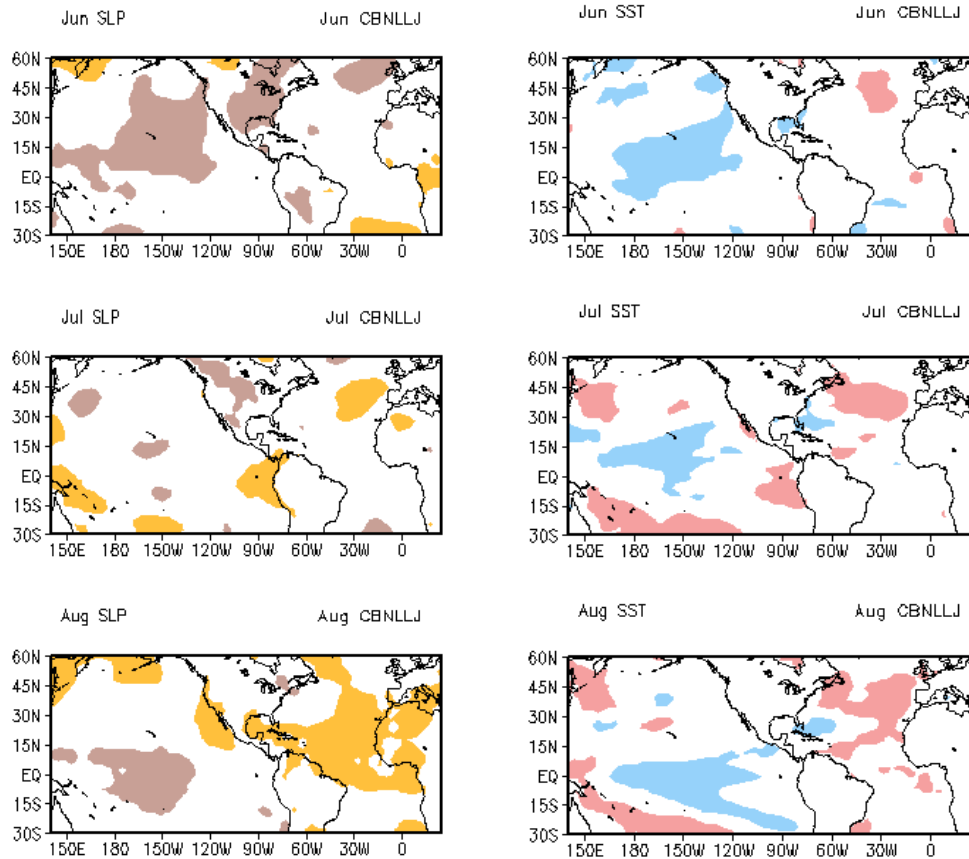


**Figure 5.14. Regions of 80% significant difference (shaded) between the correlations for the periods 1958-1978 and 1979-2001 for SLPAs and CBNLLJ (left) and SSTAs and CBNLLJ (right).**

In the Pacific, the standard deviation of the Niño3.4 index in June (July) increased from 0.55°C (0.60°C) to 0.80°C indicating that in June and July the Niño3.4 anomalous events have become more potent (i.e., greater magnitude). This increase in standard deviation of June-July Pacific anomalies is also observed from Tahiti SLP station data (Figure 5.15). By having extreme events with greater magnitude and frequency, the Pacific anomalies have a greater influence on remote regions (such as the Caribbean and tropical North Atlantic) and its influence extends to the latter part of the summer (August and September).

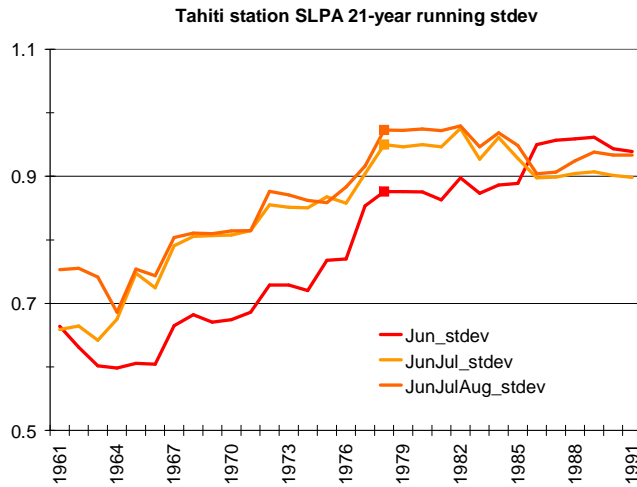


**Figure 5.15. June, June-July and June-August 21-year running standard deviation of Tahiti station SLPAs. The square on each line indicates the value for the 21-year period centered on 1978.**

In the North Atlantic, the Atlantic Multi-decadal Oscillation (AMO) was in a cooling phase throughout the 1960's and 1970's. Also the AMO changed phase more rapidly (at a rate of about 5 years) during the 1980's and 1990's reaching a significant correlation with the 5-year smoothed CBNLLJ in the 21-year period centered on 1982 and 1986. Hence, lower pressure in the tropical North Atlantic as a result of a warm AMO would have weakened the CBNLLJ.

## Chapter 6 : Conclusions

### 6.1 Climatological features

This study has analyzed the climatological features of the low-level jet over the Caribbean region and the potential mechanisms that control it. The characterization has been done mostly from the NARR with high spatial and temporal resolutions. The CBNLLJ is an extension of the anticyclone of the subtropical North Atlantic (the Bermuda High) and its northeasterly Atlantic trades are amplified by temperature and orographic influences in the Caribbean region. The Caribbean low-level wind has peaks in February and July and has minima in May and October presenting a semi-annual cycle that is in phase with the semi-annual cycle of the northward gradient of pressure across the Caribbean Sea.

The CBNLLJ's peaks of July and February have a similar vertical structure to other LLJs with a relative minimum close to the surface, a maximum at about 925 hPa and decreasing winds with height. The core of the CBNLLJ lies at 925 hPa between 12-16°N and 71-76°W. The diurnal variability of the CBNLLJ in February and July has a semi-diurnal cycle with a nighttime maximum 1.2 times the afternoon minimum, which is not as strong as the diurnal variability of the GPLLJ. Comparing the diurnal, seasonal and interannual variability of the CBNLLJ, the seasonal variability is the one that dominates.

In addition to stronger northward gradients of pressure in February and July there are regional thermal gradients that intensify the wind. From the central Caribbean to the south there is a southward air temperature gradient which may be a combination of the influence of the mountains (land) heating to the south and of cooling associated

with a minimum of precipitation over the central Caribbean. The southward temperature gradient (orthogonal to the main flow) provides a baroclinic structure to which the easterly wind would intensify. The friction closer to the surface weakens the winds at the lower levels exhibiting then a maximum away from the surface (at 925 hPa).

The moisture flux across the central Caribbean also has a jet structure in February and July. Over the central Caribbean, a spatial minimum in precipitation is correspondent to subsidence, moisture flux divergence and diabatic cooling over the Caribbean Sea. Downwind of the maximum winds of the CBNLLJ, the bifurcation of the moisture flux indicates more moisture flux to the north in July than in February. It is throughout the warm season, from May to September, that the moisture flux from the Caribbean region into the Gulf of Mexico is strongest.

The strengthening of the winds over the Caribbean Sea from May to July is influenced by the changes associated with the evolution of the rainy season in Central America and the northward displacement of the ITCZ. In combination with the divergence from the Central American monsoon area, a region of upper-level (250 hPa) convergence and stronger descent is located over the Sargasso Sea. The accumulation of mass in this tropical North Atlantic region would lead to greater pressure. The region of subsidence is collocated with a region of stronger rotational wind and lower-level divergence over the tropical North Atlantic and the Caribbean Sea.

Also, the establishment of an east-west gradient of diabatic heating between Central America and the Caribbean (as the Caribbean mid-summer drought evolves)

is related with a stronger easterly irrotational wind that results in a strengthening of the CBNLLJ. The intensification of the CBNLLJ from May to June and the stronger subsidence over the leeward (western) side of Central America influence the onset of the mid-summer drought over western Central America.

## 6.2 Interannual variability and changes

On inter-annual timescales the CBNLLJ is forced by gradients of SLPA and SSTA between the tropical Pacific and the tropical Atlantic. Basically, a weaker CBNLLJ is due to a decrease in the meridional SLP gradient across the Caribbean Sea. This weaker gradient is part of a larger-scale pattern with higher-than-average SLP in the tropical Pacific and lower-than-average SLP in the tropical Atlantic (including the Caribbean basin).

In addition to a weaker inter-basin SLPA gradient there is a concurrent inter-basin SSTA gradient. A weaker CBNLLJ is related to a warmer tropical Atlantic and a cooler tropical Pacific. On interannual timescales the influence is then from tropical anomalies. The June CBNLLJ anomalies, however, are influenced by tropical North Atlantic (TNA) SSTAs and not by an inter-basin SSTA gradient. On decadal timescales, an AMO relation is present.

These inter-basin SLPA and SSTA gradients have changed with epoch and, as a consequence, the CBNLLJ has also changed on decadal timescales. By analyzing separately the periods 1958-1978 and 1979-2001 it is concluded that the inter-basin gradients have become more influential for the latter period than for the earlier period. In fact, it has been after the late 1970's when the Pacific and Atlantic SSTAs and SLPAs became anti-correlated indicating a change in the variability of the basins.

This anti-correlation of Pacific and Atlantic SST and SLP anomalies throughout the boreal summer has induced longer extreme CBNLLJ events. The change in the CBNLLJ anomalies has been particularly outstanding in the August variability. That is to say, the August CBNLLJ extremes have become in phase with the July and September CBNLLJ extremes, with the consequence of longer CBNLLJ anomalous events.

In fact, the inter-basin patterns that Muñoz et al (2007), Wang (2007) and Whyte et al (2007) indicate to be related to the CBNLLJ had a different significance before the 1980's. The observation of an inter-basin pattern for the entire 1958-2001 period may be a result of the bias introduced in the regression and correlation by the stronger and weaker events of the latter part of the 20<sup>th</sup> century.

A notable change in the Pacific has been the standard deviation of tropical Pacific SST and SLP anomalies in June-July. After the late 1970's the tropical Pacific SSTAs have had greater standard deviation; and indication of more extreme and variable events. However, this could be an indication of the changes in the observing system after 1978. Nonetheless, there are signs of a climate shift in the late 1970's (Miller et al, 1994). This has been observed for the boreal spring Niño3.4 anomalies (Figure 6 of Munnich, 2005). Also, the interannual variability changes of the SLPA from Tahiti station data (shown in the previous chapter) and the COADS zonal wind variability in the Caribbean confirm the results from the reanalyses data.

In the North Atlantic, the NAO does not have a consistent influence on the CBNLLJ anomalies. On the other hand, the AMO modulates the CBNLLJ on a lower frequency, i.e., a decadal timescale. That is to say, a warm phase of the AMO



decreases the pressure in the tropical North Atlantic and in turn weakens the CBNLLJ through modulation of the Caribbean meridional pressure gradient.

Longer and greater magnitude summer CBNLLJ events are important in their effect on the Caribbean climate variability. The inter-basin pattern of SSTA and SLPA associated with the CBNLLJ is similar to the one observed by Giannini et al. (2000) associated with greater precipitation over the Caribbean and Central America region in July-August. In fact, the CBNLLJ modulates the precipitation anomalies in the Caribbean basin as Magaña (2000) hypothesized and Whyte et al. (2007) confirmed. Through the analyses in the present study I conclude that a weaker CBNLLJ is associated with a weaker wind vertical shear (between low-level wind and winds aloft), with weaker moisture flux divergence and with stronger precipitation. Hence, since the precipitation in the Caribbean region increases as the CBNLLJ weakens, a longer and weaker CBNLLJ would allow greater precipitation. Aside from this, the partition of the Caribbean rainy season into early (May-July) and late (August-October) rainy season (as Taylor et al. (2002) did) would be blurred by the extensions of the July Caribbean interactions into August.

### 6.3 Future work

Further study on the relationship between the CBNLLJ diurnal cycle and the precipitation diurnal cycle in the Caribbean region is necessary. This study has documented a diurnal cycle of the CBNLLJ with a nighttime maximum that is 1.2 times the afternoon minimum. Although the CBNLLJ diurnal cycle is not as large as the diurnal cycle of the mid-latitude jets, it may be important for the Caribbean precipitation.

A main finding of this study is that the Caribbean region has a southward gradient of temperature that is inductive of stronger easterly flow at the lower levels. This thermal wind effect should be validated with modeling experiments. A way to validate the influence of the land on the air temperature is by performing modeling experiments with and without the surrounding mountains and land masses. Modeling experiments would also allow the examination of a Bernoulli effect imposed by the mountains to the north and south of the Caribbean.

The analyses above present a difference in the role of the Pacific or Atlantic basin on the CBNLLJ variability at different decades of the period of study. However, most of the analyses were based on reanalyses or SST gridded products which depend on number and type of observations at some point in any given moment. These become problematic when the Pacific is under scrutiny since the tropical Pacific had a paucity of observations before the 1980's. Also, in the Caribbean basin, the precipitation in the late rainy season (August-October) is stronger than in the early rainy season (May-July) perhaps making the late rainy season (and its simulated variability) more susceptible to changes in the observations. As such, confirming the conclusions reached in this study by using station data would be advantageous.

It is also necessary to study further the interannual relationship between precipitation and the CBNLLJ. Although Whyte et al (2007) listed the regions of precipitation anomalies correlated with the CBNLLJ anomalies, more discussion is necessary. Furthermore, greater understanding of how the CBNLLJ modulates the Caribbean and Central American mid-summer droughts is necessary.

## Bibliography

- Adler, R.F., and coauthors, 2003: The Version-2 Global Precipitation Climatology Project (GPCP) monthly precipitation analysis (1979-present). *J. Hydrometeor.*, 4, 1147-1167.
- Alexander, M., and J. Scott, 2002: The influence of ENSO on air-sea interaction in the Atlantic. *Geophys. Res. Lett.*, 29, doi: 10.1029/2001GL014347
- Amador, J. A., and K. Mo, 2005: The Intra-Americas Sea low-level jet. *30<sup>th</sup> Annual Climate Diagnostics and Prediction Workshop*. Oct 24-28, 2005.
- Amador, J. A., V. O. Magaña, and J. B. Pérez, 2000: The low level jet and convective activity in the Caribbean. *Proceedings of 24th AMS Conf. on Hurricanes and Tropical Meteorology*, 29 May to 2 June 2000. 4B.5
- Barnston, G., and R. E. Livezey, 1987: Classification, seasonality and low-frequency atmospheric circulation patterns. *Mon. Wea. Rev.*, 115, 1083–1126.
- Berberly, E. H., and E. A. Collini, 2000: Springtime precipitation and water vapor flux over southeastern South America. *Mon. Wea. Rev.*, 128, 1328-1346.
- Berberly, E. H., and V. R. Barros, 2002: The hydrologic cycle of the La Plata basin in South America. *J. Hydrometeor.*, 3, 630-645.
- Berberly E. H., E. M. Rasmusson, and K. E. Mitchell, 1996: Studies of North American continental-scale hydrology using Eta model forecast products. *J. Geophys. Res.*, 101, 7305-7319.
- Blackadar, A. K., 1957: Boundary layer wind maxima and their significance for the growth of nocturnal inversions. *Bull. Amer. Meteor. Soc.*, 38, 282-290.

- Bonner, W. D., and J. Paegle, 1970: Diurnal variations in boundary layer winds over the south central United States in summer. *Mon. Wea. Rev.*, 96, 735-744.
- Bosilovich, M. G., and S. D. Schubert, 2002: Water vapor tracers as diagnostics of the regional hydrological cycle. *J. Hydrometeor.*, 3, 149-165.
- Carton, J. A., and B. S. Giese, 2007: SODA: A Reanalysis of Ocean Climate, *Mon. Wea. Rev.*, in press.
- Castro, C. L., T. B. McKee, and R. A. Pielke, 2001: The Relationship of the North American Monsoon to Tropical and North Pacific Sea Surface Temperatures as Revealed by Observational Analyses. *J. Climate*, 14, 4449-4473.
- Chen, P., M. P. Hoerling and R. M. Dole, 2001: The origin of the subtropical anticyclones. *J. Atmos. Sci.*, 58, 1827-1835.
- Chen, A. A., and M. A. Taylor, 2002: Investigating the link between early season Caribbean rainfall and the El Niño+1 year. *Int. J. Climatol.*, 22, 87-106.
- Chiang, J. C. H., and A. H. Sobel, 2002: Tropical tropospheric temperature variations caused by ENSO and their influence on the remote tropical climate. *J. Climate*, 15, 2616-2631.
- Czaja A., P. van der Vaart, and J. Marshall, 2002: A diagnostic study of the role of remote forcing in tropical Atlantic variability. *J. Climate*, 15, 3280-3290.
- Enfield, D. B., and D. A. Mayer, 1997: Tropical Atlantic sea surface temperature variability and its relation to El Niño-Southern Oscillation. *J. Geophys. Res.*, 102, 929-945.

- Enfield, D. B., A. M. Mestas-Nuñez, and P. J. Trimble, 2004: The Atlantic multidecadal oscillation and its relation to rainfall and river flows in the continental U.S. *Geophys. Res. Lett.*, 28, 2077-2080.
- Giannini, A., Y. Kushnir, and M. A. Cane, 2000: Interannual variability of Caribbean rainfall, ENSO, and the Atlantic Ocean. *J. Climate*, 13, 297-311.
- Giannini, A., M. A. Cane, and Y. Kushnir, 2001: Interdecadal changes in the ENSO teleconnection to the Caribbean region and the North Atlantic Oscillation. *J. Climate*, 14, 2867-2879.
- Gill, A. E., 1980: Some simple solutions for heat-induced tropical circulation. *Quart. J. R. Meteorol. Soc.*, 106, 447-462.
- Graham, N. E., and T. P. Barnett, 1987: Sea surface temperature, surface wind divergence, and convection over tropical oceans. *Science*, 238, 657-659.
- Helfand, H. M., and S. D. Schubert, 1995: Climatology of the simulated Great-Plains low-level jet and its contribution to the continental moisture budget of the United-States. *J. Climate*, 8, 784-806.
- Holton, J. R., 1967: The diurnal boundary layer wind oscillation above sloping terrain. *Tellus*, 19, 199-205.
- Holton, J. R., 1992: *An introduction to dynamic meteorology*. 3<sup>rd</sup> ed. Academic Press. Ch. 3, pp. 73-77.
- Hurrell, J. W., Y. Kushnir, G. Ottersen and M. Visbeck, 2003: An overview of the North Atlantic Oscillation. In: *The North Atlantic Oscillation: Climatic Significance and Environmental Impact*. J. W. Hurrell, Y. Kushnir, G. Ottersen and M. Visbeck, Eds., American Geophysical Union, 1-36.

- Inoue, M., I. C. Handoh and G. R. Bigg, 2002: Bimodal distribution of tropical cyclogenesis in the Caribbean: Characteristics and environmental factors. *J. Climate*, 15, 2897-2905.
- Kalnay, E., 2003: *Atmospheric modeling, data assimilation and predictability*. Cambridge University Press, Cambridge, pp. 1-341.
- Kalnay, E., and Coauthors, 1996: The NCEP/NCAR 40-Year Reanalysis Project. *Bull. Amer. Meteor. Soc.*, 77, 437-471.
- Kaplan, A., M. Cane, Y. Kushnir, A. Clement, M. Blumenthal, and B. Rajagopalan, 1998: Analyses of global sea surface temperature 1856-1991, *J. Geophys. Res.*, 103, 18567-18589.
- Knaff, J. A., 1997: Implications of summertime sea level pressure anomalies in the tropical Atlantic region. *J. Climate*, 10, 789-804.
- Knaff, J. A., 1998: Predicting summertime Caribbean pressure in early April. *Weather and forecasting*, 13, 740-752.
- Knight, J. R., C. K. Folland, and A. A. Scaife, 2006: Climate impacts of the Atlantic Multidecadal Oscillation. *Geophys. Res. Lett.*, 33, L17706.
- Magaña, V. O., 2000: Interannual climate variability in the Mexico, Central America, and Caribbean region. *CLIVAR Exchanges*, No. 16.
- Magaña, V., and E. Caetano, 2005: Temporal evolution of summer convective activity over the Americas warm pools. *Geophys. Res. Lett.*, 32, L02803.
- Magaña, V., J. A. Amador, and S. Medina, 1999: The midsummer drought over Mexico and Central America. *J. Climate*, 12, 1577-1588.

- Malmgren, B. A., A. Winter, and D. Chen, 1998: El Niño-Southern Oscillation and North Atlantic Oscillation control of climate in Puerto Rico. *J. Climate*, 11, 2713-2717.
- Mapes, B. E., P. Liu, and N. Buening, 2005: Indian monsoon onset and the Americas midsummer drought: out-of-equilibrium responses to smooth seasonal forcing. *J. Climate*, 18, 1109-1115.
- Mesinger, F., and Coauthors, 2006: North American Regional Reanalysis. *Bull. Amer. Meteor. Soc.*, 87, 343-360.
- Mestas-Nuñez, A. M., C. Zhang and D. B. Enfield, 2005: Uncertainties in Estimating Moisture Fluxes over the Intra-Americas Sea. *J. Hydrometeor.*, 6, 696-709.
- Miller, A. J., D. R. Cayan, T. P. Barnett, N. E. Gram., and J. M. Oberhuber, 1994: The 1976-77 climate shift of the Pacific Ocean. *Oceanogr.*, 7, 21-26.
- Mo, K. C., M. Chelliah, M. L. Carrera, R. W. Higgins, and W. Ebisuzaki, 2005: Atmospheric moisture transport over the United States and Mexico as evaluated in the NCEP Regional Reanalysis. *J. Hydrometeor.*, 6, 710-728.
- Mora, I., and J. A. Amador, 2000: El ENOS, el IOS y la corriente en chorro de bajo nivel en el oeste del Caribe. *Tópicos Meteorológicos y Oceanográficos*, 7, 27-39.
- Munnich, M. and J. D. Neelin, 2005: Seasonal influence of ENSO on the Atlantic ITCZ and equatorial South America. *Geophys. Res. Lett.*, 32, L21709.
- Muñoz, E., A. J. Busalacchi, S. Nigam, and A. Ruiz-Barradas, 2007: Winter and summer structure of the Caribbean low-level jet. *J. Climate*, in press.

- Muñoz, E., A. Ruiz-Barradas, S. Nigam and A. J. Busalacchi, 2006: Variability of the Caribbean low-level jet and its related climate anomalies. May, 2006. *Eos Trans. AGU*, 87(36), *Jt. Assem. Suppl.*, Abstract A33C-04.
- Nogues-Paegle, J. and J. Paegle, 2001: American Low Level Jets: A scientific prospectus and implementation plan. pp. 1-49. [Available online at <http://www.met.utah.edu/jnpaegle/research/ALLS.html>]
- Nogues-Paegle, J., and Coauthors, 2002: Progress in Pan American CLIVAR research: Understanding the South American monsoon. *Meteorologica*, 27, 1-30.
- Paegle, J., 1998: A comparative review of South American low-level jets. *Meteorologica*, 23, 73-81.
- Peixoto, J. P., and A. H. Oort, 1992: *Physics of Climate*. American Institute of Physics, New York. Ch. 12, pp. 273-277.
- Rasmusson, E. M., 1967: Atmospheric water vapor transport and the water balance of North America: Part I. Characteristics of the water vapor flux field. *Mon. Wea. Rev.*, 95, 403-426.
- Rasmusson, E. M., 1968: Atmospheric water vapor transport and the water balance of North America: Part II. Large-scale water balance investigations. *Mon. Wea. Rev.*, 96, 720-734.
- Reynolds, R. W., N. A. Rayner, T. M. Smith, D. C. Stokes and W. Wang, 2002: An improved in situ and satellite SST analysis for climate. *J. Climate*, 15, 1609-1625.
- Rodwell, M. J., and B. J. Hoskins, 2001: Subtropical anticyclones and summer monsoons. *J. Climate*, 14, 3192-3211.



- Rogers, J. C., 1988: Precipitation variability over the Caribbean and tropical Americas associated with the Southern Oscillation. *J. Climate*, 1, 172-182.
- Saravanan, R., and P. Chang, 2000: Interaction between tropical Atlantic variability and El Niño-Southern Oscillation, *J. Climate*, 13, 2177-2194.
- Seager, R., R. Murtugudde, N. Naik and A. Clement, 2003: Air-Sea interaction and the seasonal cycle of the subtropical anticyclones. *J. Climate*, 16, 1948-1966.
- Slutz, R.J., S.J. Lubker, J.D. Hiscox, S.D. Woodruff, R.L. Jenne, P.M. Steurer, and J.D. Elms, 1985: Comprehensive Ocean-Atmosphere Data Set; Release 1, *Climate Research Program*, Boulder, Colorado.
- Smith, T. M., and R. W. Reynolds, 2004: Improved Extended Reconstruction of SST (1854-1997). *J. Climate*, 17, 2466-2477.
- Stensrud, D. J., 1996: Importance of low-level jets to climate: A review. *J. Climate*, 9, 1698-1711.
- Taylor, M. A., D. B. Enfield and A. A. Chen, 2002: Influence of the tropical Atlantic versus the tropical Pacific on Caribbean rainfall. *J. Geophys. Res.*, 107, 3127.
- Ting, M. F., and H. L. Wang, 2006: The role of the North American topography on the maintenance of the Great Plains summer low-level jet. *J. Atmos. Sci.*, 63, 1056-1068.
- Uppala, S. M., and Coauthors, 2005: The ERA-40 re-analysis. *Quart. J. R. Meteorol. Soc.*, 131, 2961-3012.
- Vera, C., 2002: VAMOS/CLIVAR/WCRP Conference on the South American Low-Level Jet. *CLIVAR Exchanges*, 7, 34-36.

- Vera, C., and Coauthors, 2006: The South American Low-Level Jet Experiment. *Bull. Amer. Meteor. Soc.*, 87, 63-77.
- Visbeck, M., E. P. Chassignet, R. G. Curry, T. L. Delworth, R. R. Dickson, and G. Krahnmann, 2003: The ocean's response to North Atlantic Oscillation variability. In: *The North Atlantic Oscillation: Climatic Significance and Environmental Impact*. J. W. Hurrell, Y. Kushnir, G. Ottersen and M. Visbeck, Eds., American Geophysical Union, 113-146.
- Wang, C., 2005: ENSO, Atlantic climate variability, and the Walker and Hadley circulations. In: *The Hadley Circulation: Present, Past, and Future*. H. F. Diaz and R. S. Bradley, Eds., Kluwer Academic Publishers, 173-202.
- Wang, C., 2006: An overlooked feature of tropical climate: Inter-Pacific-Atlantic variability. *Geophys. Res. Lett.*, 33, L12702.
- Wang, C., 2007: Variability of the Caribbean low-level jet and its relations to climate. *Clim. Dyn.*, in press.
- Wang, C., and D.B. Enfield, 2001: The tropical Western Hemisphere warm pool. *Geophys. Res. Lett.*, 28, 1635-1638.
- Wang, C., and D. B. Enfield, 2003: A further study of the tropical Western Hemisphere warm pool. *J. Climate*, 16, 1476-1493.
- Wang, C., and S.-K. Lee, 2007: Atlantic warm pool, Caribbean low-level jet, and their potential impact on Atlantic hurricanes. *Geophys. Res. Lett.*, 34, L02703.
- Wang, C., D. B. Enfield, S.-K. Lee and C. W. Landsea, 2006: Influences of the Atlantic warm pool on Western Hemisphere summer rainfall and Atlantic hurricanes. *J. Climate*, 19, 3011-3028.

- Weaver, S. J., and S. Nigam, 2007: Variability of the Great Plains Low-Level Jet: Large-scale circulation context and hydroclimate impacts. *J. Climate*, in press.
- Wexler, H., 1961: A boundary layer interpretation of the low-level-jet. *Tellus*, 13, 368-378.
- Whyte, F. S., M. A. Taylor, T. S. Stephenson and J. D. Campbell, 2007: Features of the Caribbean low level jet. *Int. J. Climatol.*, in press.
- Xie, S-P., H. Xu, W. Kessler and M. Nonaka, 2005: Air-sea interaction over the eastern Pacific warm pool: Gap Winds, Thermocline Dome, and Atmospheric Convection. *J. Climate*, 18, 5-20.
- Xie, P., and P.A. Arkin, 1997: Global Precipitation: A 17-Year Monthly Analysis Based on Gauge Observations, Satellite Estimates, and Numerical Model Outputs. *Bull. Amer. Meteor. Soc.*, 78, 2539–2558.